Source apportionment of atmospheric aerosol in a marine dusty environment by Ionic/composition Mass Balance (IMB)

João Cardoso[1,2], Susana M. Almeida[3], Teresa Nunes[1], Marina Almeida-Silva[3], Mário Cerqueira[1], Célia Alves[1], Fernando Rocha[4], Paula Chaves[3], Miguel Reis[3], Pedro Salvador[5], Begoña Artiñano[5], Casimiro Pio[1]

[1]CESAM & Dep. Environ, Aveiro University, Aveiro, 3810-193, Portugal
[2]Cape Verde University, Praia, 279, Cape Verde
[3]C[2]TN, Instituto Superior Técnico, Lisbon University, Bobadela, 2695-066, Portugal.
[4]Geobiotec & Dep. Geosciences, Aveiro University, Aveiro, 3810-193,Portugal
[5]Environ Dep, CIEMAT, Madrid, 28040, Spain

Correspondence to: Casimiro Pio (casimiro@ua.pt)

Abstract. PM_{10} aerosol was sampled in Santiago, the largest island of Cape Verde, for one year, and analysed for elements, ions and carbonaceous material. Very high levels of dust were measured during the winter months, as a result of the direct transport of dust plumes from the African continent. Ionic and Mass Balances (IMB) were applied to the analysed compounds, permitting the determination of 6-7 different processes and source contributions to the aerosol loading: insoluble and soluble dust, sea-salt, carbonaceous material and secondary inorganic compounds resulting from the reaction of acidic precursors with ammonia, sea-salt and dust. The mass balance could be closed by the consideration and estimation of sorbed water that constituted 20-30% of the aerosol mass. The balance methodology was compared with Positive Matrix Factorization (PMF), showing similar qualitative source composition. In quantitative terms, while for Soil dust and Secondary Inorganic Compounds source classes, the results are similar, for other sources such as sea-salt spray there are significant differences in periods of dust episodes. The discrepancies between both approaches are interpreted with basis on calculated source profiles. The joint utilization of the two methodologies, which are complementary, gives confidence in our capability for the correct source apportionment of aerosol particles.

1 Introduction

The atmospheric aerosol has an important role in atmospheric physics and chemistry (Lohmann and Feichter, 2005; Poschl, 2005) and significant impacts on climate (Buseck and Pósfai, 1999; Ramanatham et al., 2001) and human health (Pope, 2000; Brunekreef and Fosberg 2005; Tobias et al., 2011).

Atmospheric aerosol is both the result of gas-to-particle transformation from natural, or anthropogenically, induced precursors and of direct emissions from the Earth's surface by the action of wind on soil and water. Gas-to-particle transformation gives fundamentally fine (sub-micrometre) particles, while wind-induced mechanic processes on the planet's surface originate mostly coarse particles, as sea-salt over the oceans, or soil dust over deserts and other bare soil areas (Seinfeld and Pandis,

1998). On a global scale, sea-spray and dust are highly dominant, in terms of suspended mass and regions affected, by comparison with other aerosol sources (Raes et al., 2000; Tanaka and Chiba, 2006). Although mostly natural, coarse aerosol particles associated with dust emissions are frequently affected by anthropogenic activities such as industry, transportation and agricultural practices, at urban and regional/hemispheric scales (Almeida et al., 2006a; Ginoux et al., 2012).

It is important to know quantitatively the sources of atmospheric aerosols in order to correctly implement strategies and measures to control and reduce atmospheric particulate pollution and its effects on nature and humankind. There is an array of methodologies to evaluate the impact of sources and precursors on atmospheric particulate loading that range from emission, dispersion and transport modelling, to source apportionment techniques (Blanchard, 1999). Source apportionment techniques use information on aerosol atmospheric composition and concentrations, at one or several locations, to infer quantitatively the sources and processes responsible for the particulate loading at the receptor (Almeida et al., 2006b; Belis et al., 2013).

In source apportionment, when the number and composition of the sources are unknown, multivariate analysis, based on particulate composition variability at the receptor(s) as a function of time, is a very common and useful methodology to quantitatively evaluate the main sources of atmospheric particulate matter (Ashbaugh et al., 1984; Henry et al., 2004; Hopke, 1985). Presently the most used multivariate analysis methodology is Positive Matrix Factorization, (PMF), because it allows the discrimination of only positive values in both source profiles and contributions (Paatero and Tapper, 1994; Paatero, 1999; Reff et al., 2007; Amato et al., 2016).

Source apportionment multivariate methodologies permit frequently to identify the impact of the majority of direct sources and gas-to-particle conversion processes and their variability in time, during the aerosol measured period. If associated with statistical backward trajectory analysis the method also permits the determination of source regions during regional and, principally, long-range transport (Salvador et al., 2016).

Multivariate methods, although very useful, are not perfect and have uncertainties resulting from collinearity of sources, the evolution of composition during transport, etc., that need to be detected and estimated (Belis et al., 2013). When a large number of compounds and elements is determined by chemical analysis of aerosol samples, an alternative methodology can be used to infer the total aerosol composition, which takes into account that the total aerosol mass is the sum of the mass of the individual components. Also from the chemical analysis, it is possible to inter-compare analysed anions and cations, which have to obey the principle of electro-neutrality. From the mass and ionic composition, it is frequently viable to infer quantitatively the origin of the aerosol, because many of the analysed constituents are tracers of specific sources.

Ionic and Mass Balances (IMB) rely mostly on the direct measurement of aerosol constituents and therefore are less affected by indemonstrable assumptions, as it happens in the assignment of the number of factors and their identities, in multivariate methods, such as PMF (Belis et al., 2014). Mass balance has been frequently applied in the past but mostly as a screening tool (Watson et al., 2002). However, if properly applied, ionic and mass balances have the potential to correctly perform the source apportionment of atmospheric aerosol. We would like to emphasize that the "European Guide on Air Pollution Source Apportionment with Receptor Models" (Belis et al., 2014) exhorts to use Receptor Models in combination with independent methodologies to achieve more robust estimations by mutual validation of the outputs. Our objective in this paper is thus, to

develop and apply a detailed ionic and mass balance to aerosol particles in a dusty marine environment, demonstrating the capability of this methodology to determine the aerosol sources with an accuracy as good as that of the most developed multivariate methods, such as PMF.

2 Mass balance methodologies

Composition and mass balance is feasible when the main components of the aerosol sources, such as soil elements, sea-salt constituents, inorganic water soluble ions and carbonaceous mass, are measured and quantified (Sciare et al., 2005; Guinot et al, 2007; Grigoratos et al., 2014; Genga et al., 2017). Even when there is a thorough quantification of aerosol constituents, it is not often possible to apportion more than 70 to 80% of measured aerosol total mass, because important elemental constituents of particulate matter, such as oxygen, in water, soil and organic carbon, are not usually analysed (Malm et al.,1994, Andrews et al., 2000; Rees et al., 2004; Perrino et al., 2013; Grigoratos et al., 2014). Oxygen is the most abundant element in the Earth's crust constituting on average 47% of the continental crust mass (Wedepohl, 1995).

For mass balance purposes, the determination of soil contribution is, usually, inferred from the analysis of the major soil elements measured in the aerosol samples (Si, Al, Fe, Mn, Ti, etc.), taking into account the presence of their oxides:

Soil Dust Mass= SiO_2+Al_2O_3+Fe_2O_3+MnO+TiO_2+etc.. Equation 1

Depending on the completeness of the soil elemental analysis and the composition knowledge of the source soils, it is possible to adapt the above equation to better apportion the soil mass by mass balance (Formenti et al., 2001; Eldred, 2003; Andrews et al., 2000, and references there in):

Soil Dust Mass= F(2.14Si+1.89Al+1.43Fe+1.39Mn+1.67Ti+etc.), Equation 2

where F is a multiplying factor that takes into account the unmeasured material (such as elements and the presence of hydrated water) in the soil dust.

The sea-salt contribution is evaluated by considering that emitted sea-salt spray has the composition of salt in sea-water. A possible exception is chloride that frequently appears in lower ratios due to sea-salt spray interaction with atmospheric acids, such as HNO_3, H_2SO_4, or SO_2, which results in the evaporation of Cl^-, as HCl. The Cl^- in the particulate phase can be, partially, or totally, substituted by NO_3^-, or SO_4^{2-}, in the form of secondary sodium and magnesium nitrates and sulphates (Pio and Lopes, 1998). A similar reaction can take place between these atmospheric strong acids and dust, resulting, for example, in the partial or total vaporisation of carbonates, as CO_2, and the formation of secondary calcium nitrates and sulphates (Pio et al., 1994; Goodman et al., 2000).

Soil carbonates are part of the carbonaceous aerosol. As they are, infrequently, analysed, in source apportionment they have to be approximately inferred from calcium and magnesium measurements. In dusty environments, the measurement of carbonates is important to permit a more correct composition/mass balance source apportionment.

Another component of the carbonaceous aerosol is the organic mass. This component is usually calculated from the measurement of organic carbon, by applying a multiplication factor to take into account other unmeasured elements such as

nitrogen, sulphur and, principally, oxygen. Factors ranging from 1.2 to 2.3 have been employed for this purpose (Countess et al., 1980; Japar et al., 1984; Rogge et al., 1993a; Rogge et al., 1993b; Sempere and Kawamura, 1994; Russel, 2003; Chen and Yu, 2007; El-Zanan et al., 2009). The highest values are commonly used in sites affected by biomass burning emissions, rich in sugars and organic acids, or away from emission sources, because under these conditions the precursor organic material had plenty of time to be strongly oxidised (Turpin and Lim, 2001; Sciare et al. 2005; Ervens et al., 2011). Genga et al., (2017) used variable values between 1.8 and 2.1, depending on the direction of the wind, to best fit the mass closure process, in a Mediterranean Port city.

Water is a common and important component of atmospheric aerosol that may constitute up to 20% of the total PM mass (Canepari et al., 2013; Perrino et al., 2013). Model calculations estimate that particle-bound water constitutes 20–35% of the annual mean European atmospheric PM concentrations (Tsyro, 2005). In spite of that, only in a few studies aerosol particulate water has been indirectly or directly estimated (Dick et al., 2000; Rees et al, 2004; Stanier et al., 2004; Speer et al., 1997; Speer et al., 2003; Kitamori et al., 2009).

Several attempts have been done and published, to account for water in sampled aerosols. Using a thermodynamic equilibrium ion modelling, temperature, humidity and inorganic ions concentrations, Chen et al. (2014) estimated that water constituted up to 38% of the $PM_{2.5}$ mass in the heavily polluted atmosphere of Beijing, for aerosols weighted at 40% relative humidity (RH). To estimate strongly bound water, Harrison et al. (2003), in samples weighted at 45-50% RH, applied a hydration multiplication factor of 1.29 to the measured sulphates and nitrates (as ammonium or/and sodium compounds). Sciare et al. (2005) and Genga et al. (2017) successfully used this methodology to close the mass balance in Mediterranean aerosols.

During laboratory studies with water and sea-salt particles, Tang et al. (1997) found the presence of a hysteresis super saturation when decreasing relative humidity, with suddenly efflorescence at 47% RH. Depending on whether the particles were in a dry, or wet state, the ratio water/dry sea-salt masses observed at 50% RH was 0.4, or 1.4, respectively.

Tang and Munkelwitz (1994) and Shu et al. (1998) determined the water content in ammonium sulphate. A water/salt ratio of 0.4 was obtained at 50% RH, in liquid meta-state equilibrium. A ratio of 0.45 was employed to calculate the water contribution to ammonium sulphate aerosols by Speer et al. (2003).

Speer et al. (2003) also estimated the water content in organic aerosol particles. A relationship between the excess liquid water and the measured organic carbon mass was found. Through modelling it was determined that, on average, about 80% of the liquid water in the $PM_{2.5}$ could be accounted for by inorganic ions, with the remaining 20% associated with organic compounds. The liquid water to organic carbon mass ratio, at 50%, was estimated as 0.2 (an OM/OC=2 was considered).

3 Experimental

The present work uses data from the field campaign of the CVDUST Project, which took place in Santiago Island, Cape Verde, between January 2011 and January 2012. Atmospheric aerosol and ancillary measurements were performed on the roof platform of the Cape Verde Meteorological Institute, on the outskirts of Praia city (14.92N; 23.48W), 98 meters above sea

level and approximately 1.7 kilometres from the sea border. During the sampling period, daily averaged temperatures and RH ranged from 21 to 29 °C and from 50 to 86%, respectively. Total rainfall was only 152mm, concentrated in the months of August to October.

PM_{10} aerosol particles were collected, in parallel, onto three filter types (quartz fibre, Teflon and Nuclepore membranes) with high volume and low volume samplers, equipped with PM_{10} inlets. A total of 140 events were sampled, with filtering periods ranging from 6 to 96 hours (the low sampling periods during Saharan dust episodes) allowing the collection of enough aerosol material for all necessary analysis without the risk of clogging the filters during dust storms. Taking into account the variable extension of sampling periods, in this publication all the calculated concentration averages are weighted by the sampling time. Details of sampling and filter analysis are given elsewhere (Almeida-Silva, 2014; Salvador et al., 2016); here we only provide a summary of published information. Filters were weighted with semi-micro, or micro, balances to determine PM_{10} total mass, at 50% RH and 20°C. Mass concentrations measured in the three parallel sampling lines compared quite well, (R=0.99; best-fit lines with y/x=0.98-1.02 – for details consult Figure A1 in Annex), a confirmation that the filters were sampling the same aerosol population.

Nuclepore filters were employed to determine particulate elemental content using Particle Induced X-Ray emission (PIXE) and/or k_0-Instrumental Neutron Activation Analysis (k_0-INAA) (Almeida et al., 2013; Almeida-Silva, 2014). A total of 26 elements was measured by the two techniques, although some light elements, such as Na and Cl, could only be quantified with large uncertainties, characteristic of the analytical conditions and techniques.

The quartz filters were used to determine carbonates by acid evolution and non-dispersive infrared analysis of evolved CO_2 (Pio et al., 1994), and elemental carbon (EC) plus organic carbon (OC), with a homemade thermo–optical carbon analyser, after pre-removal of carbonates with HCl fumes, (Pio et al., 2011).

Water-soluble anions and cations, sampled in Teflon filters, were measured by ion chromatography. The method permitted the quantification of NH_4^+, Na^+, Mg^{2+} and K^+ cations, and SO_4^{2-}, NO_3^-, and Cl^- anions. Comparison between total cation and anion equivalents indicate a clear excess of cations (42%, on average). Inclusion of independently measured carbonates in the ionic balance, brings the ratio cations/anions to 0.93, demonstrating the importance of carbonate measurements for a more complete aerosol characterisation in dusty environments (see Figure A2 in Annex, for details).

4 Results and discussion

4.1 PM_{10} mass and components

As reported elsewhere (Almeida-Silva, 2013; Pio et al., 2014; Salvador et al., 2016) Cape Verde has two distinct atmospheric pollution seasons. During winter months (December-February) the atmospheric boundary layer is impacted by important dust intrusions from the Saharan region, with daily averaged PM_{10} concentrations going up to hundreds of $\mu g.m^{-3}$ (see Figure 1 and Table 1); This period is locally designated by “Bruma-Seca”, meaning “Dry-Haze”.

During May-September there is no direct intrusion of dust plumes from Africa, at lower atmospheric levels, in the boundary layer, (represented by a blue shade mask in Figure 1), and we call it "Dust-Free" season. During the "Dust-Free" period the atmosphere contains still important quantities of dust, originated, either from the island arid surface, or from continuous dust transport from Africa into the region across the free troposphere, which partially sediments to lower atmospheric levels (Gama et al., 2015). The months of March, April, October and November have intermittent direct intrusions of Sahara dust, with PM_{10} concentrations sometimes reaching one hundred $\mu g.m^{-3}$. Throughout this document we present average results for the total sampling period and for the two "Dry-Haze" and "Dust-Free" seasons.

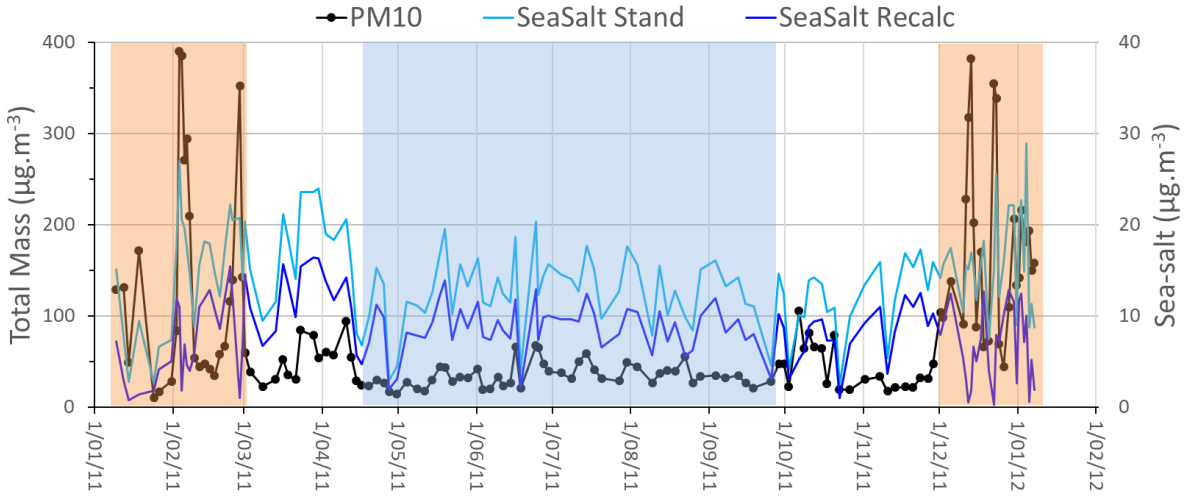

Figure 1: Levels of PM_{10} and sea-salt along the annual sampling period. Shades of brown and blue represent, respectively, periods clearly with (Dry-Haze) and without (Dust-Free) dust plume direct intrusions. "SeaSalt Stand" are concentrations of sea-salt spray calculated by considering Na^+ as an exclusive tracer of marine emissions. "SeaSalt Recalc" represent sea-salt levels estimated after removal of soil dust Na^+ and Mg^{2+}.

4.2 Sea-salt and soil sources

PM_{10} in Cape Verde is mainly influenced by emissions from sea and soil surfaces (Gama et al., 2015). The determination of the soil contribution, by composition/mass balance, can be improved from the knowledge of source soil composition. When information on dust originated soil is unavailable, average global upper continental crust composition is frequently employed (Manson and Moore, 1982; Wedepohl, 1995). In our case, dust is almost exclusively originating from North African Sahara and Sahel, and information on regional soil composition for these regions is available.

There is a handful of publications on soil composition in North Africa, which provide evidence of a wide composition variability across the Saharan and sub-Saharan regions (Guieu et al., 2002; Journet et al., 2013; Scheuvens et al., 2013, and references there in). One of the most complete Saharan soil data sets was given by the IDEA-CSIC Research Group (Moreno

et al., 2006). The publication provides the concentrations of 47 elements in the bulk soil of 9 locations, across four regions, in North Africa (Hogar Massif, Chad Basin, Niger and Western Sahara). Castillo et al. (2008) provides soil size distributed composition information for the same sites. We used this data set to infer the composition and mass balance of soil dust in our samples (Table A1, in Annex, adapted from Moreno et al., (2006), shows compound average contributions).

Saharan soil composition in Moreno et al. (2006) reveals some differences by comparison with the average crust/upper crust (Manson and Moore, 1986; Wedepohl, 1995), with a relative enrichment of Si and Ti, probably as a result of intense weathering of Sahara desert soils. Si and Ti form rather hard crystals (silica and rutile), resistant to physical weathering. The size chemical speciation of Saharan soils by Castillo et al. (2008) revealed Al, Mg, and Fe moderate enrichments, in suspended finer particles, in opposition to K that had increased concentrations at coarser sizes.

Table 1: Weighted average concentrations of PM_{10}, major elements, ions and carbon fractions, for the total campaign and for Dry-Haze and Dust-Free seasons. Na and Cl (in red) were measured with important inaccuracies, as evidenced by comparison with the respective water-soluble ion concentrations.

	Year Average ($ng.m^{-3}$)	Dry-Haze ($ng.m^{-3}$)	Dust-Free ($ng.m^{-3}$)
PM10	59,602	117,000	33,900
Si	6,595	17,100	2,150
Al	3,814	9,930	1,220
Na	3,230	3,440	3,040
Fe	1,835	4,560	721
Ca	1,450	2,920	783
Mg	969	2,130	454
K	772	1,580	380
Ti	197	454	93
Ba	31	66	21
Mn	31	78	12
Cl	4,660	5,810	3,930
S	852	941	792
Na^+	4,047	4,360	3,760
Ca^{2+}	818	1,540	475
Mg^{2+}	386	443	351
K^+	240	251	166
NH_4^+	213	101	257
Cl^-	5,344	5,770	4,840
SO_4^{2-}	1,898	1,880	1,880
NO_3^-	1,191	1,250	115
CO_3^{2-}	816	2,230	169
EC	188	110	270
OC	980	1,340	870

Aerosols generated by suspension from Sudan desert soil, have also shown an Al enrichment, while there has been an impoverishment in Si and Ti elements, in smaller particles (Eltayeb et al., 2001). The ratio Al/Si in suspended dust decreased with increasing particle size. A similar behaviour happened to the ratio Al/Ti, for particles <45 µm. The authors attributed this behaviour to the presence of large quartz crystals in soil and their substitution in dust by smaller particles of alkali-plagioclase and clay minerals.

Journet et al. (2014) concluded that, in desert soils, silica minerals accumulate preferably in the silt fraction (2µm<Dp<65µm), while kaolinite and other clay minerals are mostly concentrated in the clay size fraction (Dp<2µm); kaolinite that has a ratio Al/Si=0.95 is the main mineral of desert areas. The authors assumed that the mineral composition of airborne dust is broadly similar to that of the clay size fraction in the desert soil.

Taking into account the previous information we speculate that, as a result of soil weathering, particles containing Si are heavier/larger than other soil particles and, therefore, are more difficultly suspended by the wind and exported to other regions, enriching local soils.

Consequently, it is expectable that Saharan suspended dust will be impoverished in Si and Ti, by comparison with less hard minerals containing Al, Fe, Mg, Na, etc. This is observed in our aerosol samples where there is a quite constant Al/Si mass ratio of 0.61, independent from the period of the year or the air mass trajectories (Al=0.61Si-254 $ng.m^{-3}$; R=0.99). Comparison between prevalently soil originated elements, showed that, for Al, Fe and Mn, the concentration ratios in the aerosol are similar to those in average crustal material and within the limits of Sahara data from Moreno et al. (2006). In contrast, the ratio between particulate Al and Si (or Ti) levels is 2 to 4 times higher than in Moreno et al. (2006), indicating a Si (Ti) deficit, by comparison with other major Saharan soil elements (for clarification see Figure A3, in Annex). After aerosol measurements performed in Southern Morocco, Kandler et al. (2006) concluded that the major dust constituents were quartz, potassium feldspar, plagioclase, calcite, hematite and clay minerals. Particles in the range of 0.5-50 µm consisted mainly of silicates and, above 50 µm, quartz was dominant.

Published information concerning the Al/Si mass ratios in atmospheric dust from the Saharan region is still scarce. Al/Si average ratios of 0.43-0.49, with values, depending on the air mass origin, were measured by Chiapello et al. (1997), using bulk filtration, in Sal Island, Cape Verde. Formenti et al. (2003) determined Al/Si ratios of the order of 0.5, in particles larger than 1 µm, during aircraft measurements performed in the Cape Verde region. Remoundaki et al. (2013) found Al/Si ratios of 0.44±0.12 in $PM_{2.5}$ aerosols collected in Greece under the influence of air mass transport from the Saharan region. In South America, Formenti et al. (2001) observed Al/Si values of 0.48±0.08 in fine particles and of 0.77±0.18 in the coarse aerosol fraction. Aerosol measurements over western Atlantic and the eastern coast of USA present an Al/Si ratio value coincident with our measurements (Eldred, 2003). From this information we hypothesise that during long-range transport of Saharan dust there is a prevalent loss, by sedimentation (or non-emission), of Si (and Ti), in comparison with other particulate dust components, which becomes more evident for larger particles.

Because of the Al/Si behaviour in our samples, we felt more confident in using Fe as a representative tracer of soil contribution in composition/mass balance calculations. In addition, Fe is the soil element that showed a better correlation (R=0.99) with PM_{10} total mass during dust events (see Figure A4, in Annex, for visualisation).

In coastal, or marine, non-dusty, environments it is common, and correct, to infer the mass contribution of particulate sea spray to the atmospheric aerosol by using Mg^{2+} or, predominantly, Na^+, as an exclusive sea-salt tracer. However, these ions are also present in the soil and, during dust episodes, the soil contribution cannot be neglected. From Figure 1 it is possible to observe that sea-salt concentrations calculated in this way increase steeply during dust pollution episodes, which is not reasonable.

To eliminate the soil interference in sea-salt estimation, we employed Fe/Mg^{2+} and Fe/Na^+ mass ratios superior edge lines (see Figure 2). Similarly to Pio et al. (2011), edge lines estimation is based on tracing a linear best fit line through the 5% of total concentration points (7 points in our case) with the highest $(Fe/(X-X_{min})$ ratios, where, presently, X is Na^+ or Mg^{2+} ion concentration and X_{min} is the respective measured minimum ion concentration. These edge lines represent the minimum fractional contribution of sea-salt to Na^+ and Mg^{2+} in the aerosol, compatible with experimental data. Therefore, it is expectable that they represent, reasonably well, the ratios between the ions and Fe, in soil dust, as long as it is acceptable that, in such a location, these are the unique major sources of Fe and Na^+. Based on these edge line ratios, the amounts of soil Mg^{2+} and Na^+ ions can thus be determined and subtracted to the total ion concentrations, permitting a first estimation of sea-salt Mg^{2+}_s and Na^+_s. As these edge lines only approximatively represent the soil ratios, the calculation of sea-salt contributions may consequently suffer from these inaccuracies/variabilities.

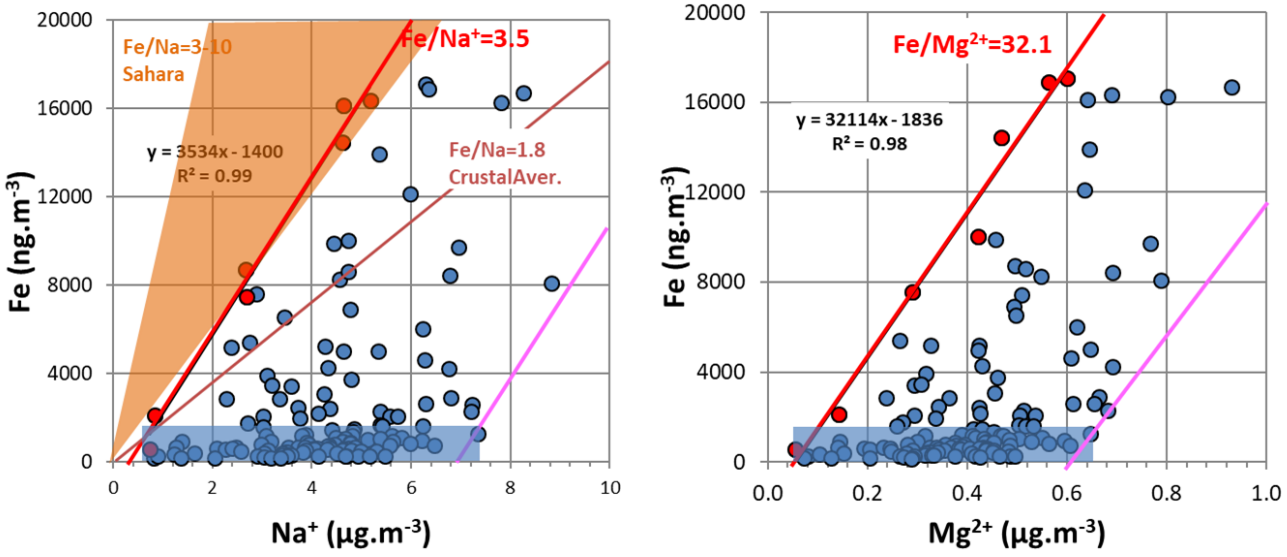

Figure 2: Edge lines (in red) for Fe versus Na^+ and Fe versus Mg^{2+} inter-comparisons. The blue rectangle represents periods without significant dust intrusions. The pink lines are parallels to the red edge lines in the maximum ion concentration regions. Also shown Fe/Na ratio ranges in Sahara and global soils, for total sodium, taken from Moreno et al., (2006), and Manson and Moore, (1982). Edge lines are best fit linear lines traced through points in red.

A further refinement of sea-salt calculation can be implemented by looking at the ratios (Na^+_s/Mg^{2+}_s), calculated from Na^+_s and Mg^{2+}_s in each sample, and comparing them with those in seawater (Mg^{2+}_{ss}/Na^+_{ss}=0.12 $\mu g.\mu g^{-1}$, Turekian, 1968). Since it is not possible to have less Mg^{2+}_{ss} (or more Na^+_{ss}) ion mass sea-salt than the one given by the 0.12 ratio, if $Mg^{2+}_s/Na^+_s \geq 0.12$, Na^+_s is chosen as the true sea salt Na^+_{ss} concentration. Otherwise, Mg^{2+}_s is chosen as the true Mg^{2+}_{ss} tracer. The contributions of other sea-salt ions are, consequently, estimated from the chosen Na^+_{ss} or Mg^{2+}_{ss}, using the salt ratios present in seawater (Turekian, 1968).

Figure 1 presents the estimation of sea-salt contribution to the aerosol ("SeaSalt Recalc"), considering the methodology described above. The Figure shows that, with the modified methodology, there is no increase of sea-salt aerosol loading during dust intrusions, in contrast with the standard methodology. During the dust periods there is, even, a decrease in the contribution of sea-salt to the aerosol that may result either from excessive calculation of soil Na^+ and Mg^{2+}, or, more probably, from an increased deposition rate of sea-salt during dusty periods, by co-sedimentation of dust and sea-salt particles. Because of the application of our adapted alternative methodology, the amount of calculated sea-salt contribution decreases by 47% in the Dry-Haze season and 32% in the rest of the year.

The correct determination of sea-salt ion concentrations permits the estimation of the remaining common elements, supposedly from soil origin. In this way, it is possible to calculate Mg_{soil}, K_{soil} and Ca_{soil} concentrations. Determination of total Na_{soil} and Cl_{soil} is not feasible in this work because of analytical limitations.

Taking into account that we did not, or could not, measure with accuracy P and Na, the calculation of soil contribution was done by adapting Equation 2 to:

$$\text{Soil Dust}=1.15(2.14Si+1.89Al+1.43Fe+1.39Mn+1.67Ti+1.66Mg_{soil}+1.40Ca_{soil}+1.20K_{soil}), \quad \text{Equation 3}$$

where the Factor 1.15 is an average for the nine sites studied by Moreno et al., (2006), (see Table A1 in Annex, for detail and clarification). This factor is higher than the corresponding values for the average continental / upper crust (1.05-1.06), taken from Manson and Moore (1982) and Wedepohl (1995).

4.3 Secondary formation processes

The attribution of analysed water-soluble anions and cations to different sources and formation processes can be done using the sequential ionic balance proposed by Alastuey et al. (2005), adapted and developed by Mirante et al. (2014) for the Madrid urban aerosol. The present situation, with very large inputs of dust and marine aerosols, imposes a further adaptation of the ionic balance method, because gas-to-particle reactions involving precursor pollutants and sea-salt spray, or dust, cannot be neglected, and, from the evaluation of dust and sea-salt composition, the amounts of soluble ions of sea-salt and dust origin have to be initially calculated. Therefore, the ionic balance applied to the present samples is the following:

1-Start by calculating soil Na^+_{soil} and soil Mg^{2+}_{soil} from Fe/Na^+ and Fe/Mg^{2+} edge lines in Figure 2.

2-Calculate sea-salt Na^+_s and Mg^{2+}_s from differences between total and soil Na^+_{soil} and Mg^{2+}_{soil}.

3-Recalculate sea-salt Na^+_{ss} and Mg^{2+}_{ss}, using minimum values and the Na^+/Mg^{2+} ratio in seawater.

4-Calculate sea-salt mass concentration and composition from Na^{+}_{ss} and Mg^{2+}_{ss}, and seawater ion ratios, taking into account available Cl^{-}.

5-Calculate non-sea-salt SO_4^{2-}, NO_3^{-} and Cl^{-}.

6-Associate, sequentially, free non-sea-salt SO_4^{2-} and NO_3^{-} with NH_4^{+}, until all NH_4^{+} is neutralized.

7-From the differences between total and sea-salt cations, calculate soil Na^{+}_{soil}, Mg^{2+}_{soil}, K^{+}_{soil} and Ca^{2+}_{soil}.

8-Associate free NO_3^{-}, sequentially, with free sea-salt and soil cations.

9-Associate, totally, CO_3^{2-}, sequentially, with free soil Ca^{2+}_{soil}, Mg^{2+}_{soil}, Na^{+}_{soil} and K^{+}_{soil}.

10-Associate free SO_4^{2-}, sequentially, with free Ca^{2+}_{soil}, Mg^{2+}_{soil}, Na^{+}_{soil} and K^{+}_{soil}

11-Associate free Cl^{-} with free Na^{+}_{soil} and Mg^{2+}_{soil}. Any excess Cl^{-} is associated with K^{+}_{soil}

12-Calculate the total masses of water-soluble soil sulphate, nitrate and chloride.

13-Edge line ratios between Fe and sulphate, nitrate, or chloride, permit a rough calculation of the fraction of these ionic compounds that are present in the soil, or that result from secondary reaction with atmospheric produced acids (for visualization see Figure A4, in Annex).

Using an Excel spreadsheet, the 13 steps were applied, sequentially, in order to attribute all measured cations and anions to sea-salt, soil and secondary inorganic compounds. The first 4 steps were described in detail in the beginning of this section. Due to space limitations, only results for the remaining 8 steps are presented.

Table 2: Soil and secondary inorganic compounds resulting from the ionic balance

					SIC ss+du			
Inorganic Compounds	**SIC am**		**SoilDust sol**		**SIC du**		**SIC ss**	
	Dust-Free	**Dry-Haze**	**Dust-Free**	**Dry-Haze**	**Dust-Free**	**Dry-Haze**	**Dust-Free**	**Dry-Haze**
	(µg.m^{-3})	**(µg.m^{-3})**	**(µg.m^{-3})**	**(µg.m^{-3})**	**(µg.m^{-3})**	**(µg.m^{-3})**	**(µg.m^{-3})**	**(µg.m^{-3})**
$(NH4)_2SO_4$	0.94	0.37						
NH_4NO_3	0.00	0.01						
$CaCO_3$			0.27	3.15				
$MgCO_3$			0.01	0.25				
Na_2CO_3			0.00	0.28				
K_2CO_3			0.00	0.00				
$NaNO_3$			086	1.26	0.75	0.60	0.43	0.16
$Mg(NO_3)_2$			010	0.12	0.09	0.06	0.08	0.03
KNO_3			0.06	0.10	0.05	0.05	0.01	0.00
$Ca(NO_3)_2$			0.01	0.00	0.00	0.00	0.02	0.01
$CaSO_4$			0.59	0.43	0.42	0.11		
$MgSO_4$			0.01	0.15	0.01	0.04		
Na_2SO_4			0.12	0.80	0.09	0.20		
K_2SO_4			0.05	0.06	0.04	0.01		
NaCl			0.27	1.75	0.17	0.68		
$MgCl_2$			0.00	0.06	0.00	0.02		
KCl			0.00	0.06	0.00	0.02		
TOTAL	**0.94**	**0.37**	**2.34**	**8.48**	**1.60**	**1.80**	**0.54**	**0.20**

Using a ratio of OM/OC=2.0 and measured EC and OC, it is also possible to estimate the total non-carbonated, carbonaceous aerosol.

With this IMB methodology, it is possible to account for the presence of seven source classes: Sea-Salt spray (SeaSalt), Insoluble Soil Dust (SoilDust ins), Soluble Soil Dust (SoilDust sol), Secondary Inorganic Compounds from the reaction of atmospheric acids with ammonia (SIC am), Sea-Salt (SIC ss) and Dust (SIC du), and non-carbonate Carbonaceous elemental and organic matter (Carbon).

The results of water-soluble compounds are presented in Table 2, for the Dry-Haze and Dust-Free seasons. Concentrations of secondary ammonium salts (SIC am) more than double during the Dust-Free season, probably as a result of higher temperatures and transport of air masses from non-desert polluted areas, or the removal by co-sedimentation with dust, during dust episodes. Soluble soil dust (SoilDust sol) more than triple during the Dry-Haze season, being formed mainly by calcium carbonates and sulphates, sodium nitrates and sulphates, and by sodium chloride.

Reaction of acid precursors with soil dust (SIC du) produces equivalent amounts of secondary compounds during the two seasons, probably because of limited availability of acidic precursors. Secondary processes resulting from acidic reactions with sea-salt (SIC ss) produce more sea-salt secondary material during the dust-free season. As, in the present conditions, it is difficult to clearly differentiate between the two processes, because it is not possible to give a priority in the competitive acidic reaction with sea-salt, or dust, in the rest of the publication the two source processes are treated together, as SIC ss+du.

4.4 Particulate water

The fractional contribution of the 6, adapted, source classes is given in Figure 3, for the two seasons and for the total campaign. The figure reveals that the sum of the quantified sources only accounts for 76% of the measured PM_{10} total mass concentration, on average, during the total measurement campaign. The value decreases to 68% during the Dust-Free season. These fractions are of the same order of values published in literature (Perrino et al., 2013; Rees et al., 2004; Andrews et al., 2000; Grigoratos et al., 2014).

As in our case carbonates were directly measured, it is predictable that most of the unaccounted mass results from the aerosol water content, in the form of adsorbed/absorbed water (hydrates in soil constituents were already considered with the application of Factor F), now that PM_{10} total mass measurement was performed at 20 °C and 50% RH, in conditions of equilibrium between the laboratory atmospheric water vapour and the particulate material in the filter.

To estimate the amount of sorbed water in the aerosol we consider that, by approximation, there is a thermodynamic equilibrium between the controlled room atmosphere, at 20°C and 50% RH, and the aerosol deposited on the filter, during the mass weighting in the Laboratory, and also that the behaviour of different compounds is independent of internal or external mixture conditions.

For sea-salt, thermodynamic information from Tang et al. (1997) was used, which, at 50% RH and 20 ºC, indicates a water/salt mass equilibrium ratio of 0.4 for a dry phase state, or 1.4 for a metastable deliquescent liquid phase state. The ISORROPIA

thermodynamic equilibrium model (Nenes et al., 1998a, 1998b) was applied, at 20ºC and 50%RH, both to the calculated sea-salt, alone, (SeaSalt) and considering, together, the sea-salt and the secondary inorganic compounds formation by the attack of atmospheric acids (SeaSalt + SIC ss). ISORROPIA output gave water fractions very similar, in both cases, and also coincident with the values taken from Tang et al. (1997) for wet or dry containing phases. As information about phase status during weighting is unavailable and the weighting was performed at RH very near the forced efflorescence point (47% RH), we used for the water/salt ratio the arithmetic average of the two equilibrium values (0.9).

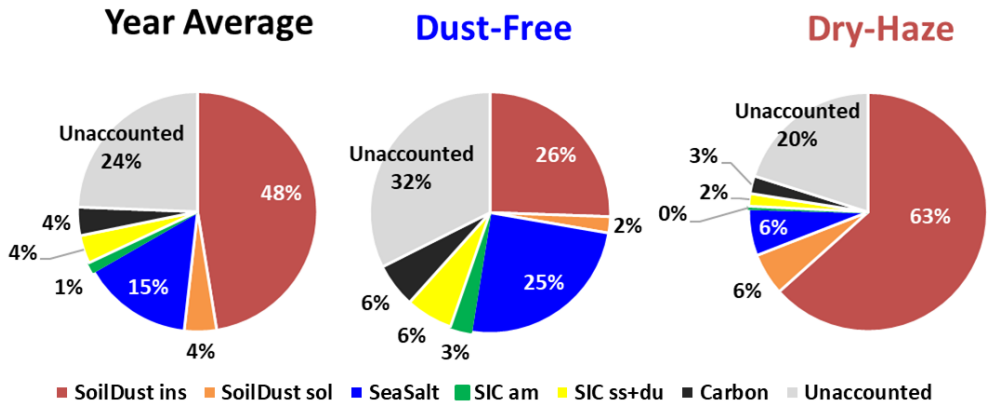

Figure 3: Contribution of different components to the PM_{10} measured total mass, estimated by IMB, for the whole sampling campaign and for the "Dust-Free" and "Dry-Haze" seasons.

For secondary inorganic water-soluble ammonium salts (mainly ammonium sulphate), thermodynamic information from Xu et al. (1998) and Tang and Munkelvitz (1994) was applied, which shows an equilibrium water/ammonium sulphate mass ratio of 0.4 at 50% RH.

The information concerning the water content of organic polar matter was taken from Speer et al. (2003) who used water/OC ratio of 0.2.

Suspended soil also sorbs water, principally the water-soluble ionic component. We used ISORROPIA, version 2.1, which includes ions from crustal origin, to estimate the water content in soluble dust. The ISORROPIA II version was run for a liquid metastable assumption and applied to the soluble soil dust (SoilDust sol) and to the sum of soluble soil dust and secondary inorganic compounds formed from the attack of atmospheric acids on dust particles (SoiDust sol + SIC du). In the first case, the average water/salt mass ratio calculated was 0.22 in the Dust-Free season and 0.47 in the Dry-Haze season. In the mixture, the calculated ratios were comparable (0.14 and 0.50, respectively). Due to the lack of more specific information, water/soluble dust ratio values of 0.2, during the Dust-Free season, and 0.5, during the rest of the year, were employed.

Various important components of the insoluble fraction of dust are hygroscopic, such as clay minerals. Schuttlefield et al. (2007) measured water adsorption by clay minerals having found a large variability in the water uptake by different clay mineral species, with water/clay mass ratios varying from 0.02-0.06 for kaolinite, going up to 0.17 for ilite and 0.08-0.7 for

montmorillonite, at 23 ºC and 50% RH. Based on these data, a round value of 0.1 for the ratio water/SoilDust ins was adopted for our samples.

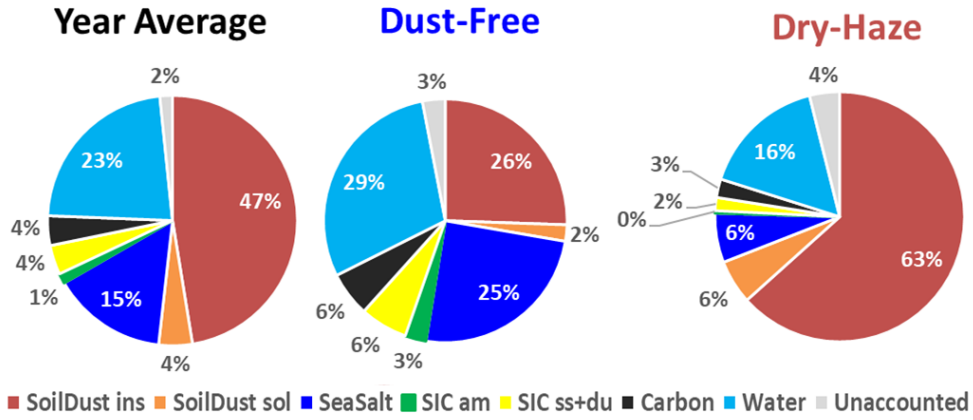

Figure 4: Inclusion of estimated water in the IMB, for the total sampling campaign and for the Dust-Free and Dry-Haze seasons.

The estimation of total water content in the collected aerosols using the above referred ratio assumptions is presented in Figure 4. The figure shows that, by using this methodology, there is almost a perfect accounting of the PM_{10} total mass. Water represents an average contribution of 23% to the aerosol mass. During the Dry-Haze period, the calculated water, on average, accounts for 16% of the PM_{10} mass, with a maximum contribution of 29% during the Dust-Free season. By including particulate water, only around 2-4% of the PM total mass is unaccounted, with the applied IMB methodology.

4.5 Comparison with PMF

The final ionic and mass balance calculations are presented in Figure 5, for the total campaign and the two seasons, considering the components associated with the respective water uptake. The addition of sorbed water reinforces the impact of hygroscopic /soluble components, such as sea-salt, in the atmospheric aerosol loading, which, for example, during the Dust-Free season increases its contribution from 25 to 47%.

The results of IMB can be evaluated and compared with PMF results applied to the same data set and already published by Salvador et al. (2016). Here, the published PMF results were reorganised, in order to explicit the PMF contributions during the two Dry-Haze and Dust-Free seasons and to show unaccounted/excess calculated PM mass, as represented in Figure 6.

The PMF analysis could differentiate 7 aerosol sources: three concerning soil contamination, two considering Secondary Inorganic Components, plus sea-salt and combustion processes. The dust sources comprised “Mineral1”, associated mainly with Al, Si and Fe, “Mineral2”, associated with CO_3^{2-} and Ca^{2+}, and “Dust+Ind” containing both soil elements (Al, Si, Fe) and tracers of industrial emissions (V, Ni, Cu and Cr). The secondary inorganic components included “SIC1”, associated with NH_4^+, SO_4^{2-}, NO_3^- Na^+, K^+ and Mg^{2+}, and “SIC2” containing SO_4^{2-}, NO_3^-, Ca^{2+} and Mg^{2+}. The “SeaSalt” source represented

most of the variability of Na^+, Cl^-, Mg^{2+}, Br and K^+. The "Combustion" source included mainly EC and OC variability (Complementary information concerning PMF sources compositions and contributions can be found in Figure A8, in the annex section).

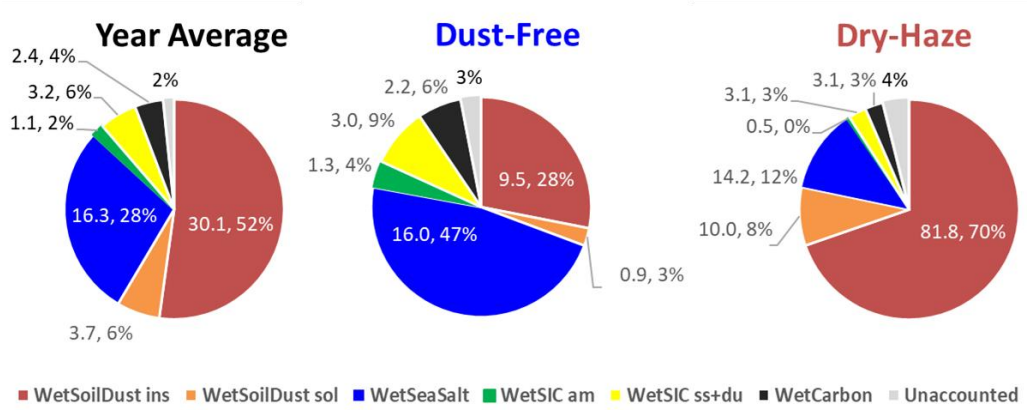

Figure 5: IMB obtained by attributing the calculated water content to the respective source classes, for the entire campaign and the Dust-Free and Dry-Haze seasons. Values are in µg.m^{-3} and percentage of measured total mass.

Table 3 compares both methodologies for the two seasons and the total campaign (for individual sampling events consult Figures A6 and A7, in Annex). There is a good agreement between the two source apportionment techniques. Both methodologies reproduce almost totally the measured PM_{10} total mass.

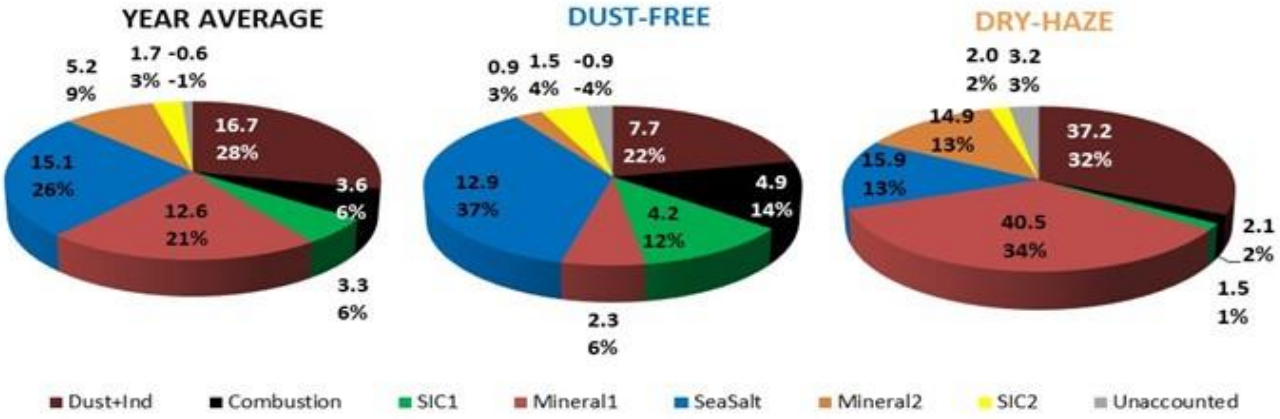

Figure 6: PMF source apportionment results, for the total campaign and during the two pollution seasons. Values are in µg.m^{-3} and percentage of measured total mass.

Table 3 shows a good comparability between total soil dust estimated by both methods in any season. In the IMB, SoilDust sol fraction is approximately equivalent to the Mineral2 component of PMF. The mass balance method could not discriminate the Dust+Ind from the total insoluble dust fraction, as was possible with PMF.

Contribution of sea-salt was also equally estimated by the two techniques, on average, during the Dry-Haze season, but during the Dust-Free free period the IMB estimated somehow higher sea-salt levels than the PMF.

SIC values are similar in both source apportionment methodologies, but during the Dust-Free period the PMF estimated higher SIC contributions. This was mainly due to higher estimations of ammonium secondary salts by the PMF, which only can happen if other compounds are included in the source component, as evidenced by the PMF source profile.

There is also a higher contribution from carbonaceous/organic/combustion material in PMF, by comparison with IMB, principally during the dry season, although a high factor of 2 was applied to the OM/OC ratio in the mass balance approach. The inclusion by the PMF of other constituents from combustion processes in West Africa is, probably, the reason for the discrepancy.

Table 3: Comparison between IMB and PMF results, grouped into four main classes. PM10 represents gravimetric measurements of total mass (in IMB, Soil=WetSoilDust ins+WetSoilDust sol; in PMF, Soil=Mineral1+Mineral2+Dust+Ind; in IMB, SIC=WetSIC am+WetSIC ss+du; in PMF, SIC=SIC1+SIC2)

	Year Average		**Dry-Haze**		**Dust-Free**	
	PMF ($\mu g.m^{-3}$)	**IMB** ($\mu g.m^{-3}$)	**PMF** ($\mu g.m^{-3}$)	**IMB** ($\mu g.m^{-3}$)	**PMF** ($\mu g.m^{-3}$))	**IMB** ($\mu g.m^{-3}$))
Soil	34.5	33.8	92.6	91.8	10.9	10.
Sea-salt	15.1	16.3	15.9	14.2	12.9	16.0
SIC	4.9	4.2	3.5	3.6	5.7	4.3
Carbon/Combust	3.6	2.4	2.1	3.1	4.9	2.2
SUM	**58.2**	**56.8**	**114.1**	**112.7**	**34.5**	**32.8**
PM_{10}	**57.7**		**117.3**		**33.9**	

Further insight into the capabilities and limitations of IMB versus PMF can be attained by comparing source classes for each individual sample, as presented in Figure 7. From this figure it is possible to confirm the good comparability between the Soil source estimations by both methods, with a linear ratio estimation of 1.04 and a correlation R=0.97.

For Sea-salt estimation, the comparison is not so good with IMB/PMF ratio estimation of only 0.68 and an R=0.82. This happens principally because, for several samples, PMF gives zero or negative Sea-salt contributions, while the IMB estimates important Sea-salt values. For a location in the middle of the ocean, it is not expectable to have absence of sea-salt and therefore, in our opinion, PMF fails, attributing, probably, the available sea-salt to a Soil source. At high concentration levels there is a tendency of PMF to give higher sea-salt values than IMB. An inspection of PMF compounds contribution to Sea-salt source shows that, in average, there is a mass inclusion of about 20% of elements such as Si, Al, Fe, etc., in this source (see

Figure A8, graph 8, for clarification). Therefore, it is clear that PMF could not completely separate Soil from Sea-salt sources, probably because of the overwhelming presence of soil during dust episodes. During the "Dust-Free" season IMB tends to give somehow higher Sea-salt contributions than PMF (Sea-salt IMB= 0.73 Sea-salt PMF+6.8; R=0.84). One of the possible reasons may be a too high estimation of sea-salt sorbed water, in IMB.

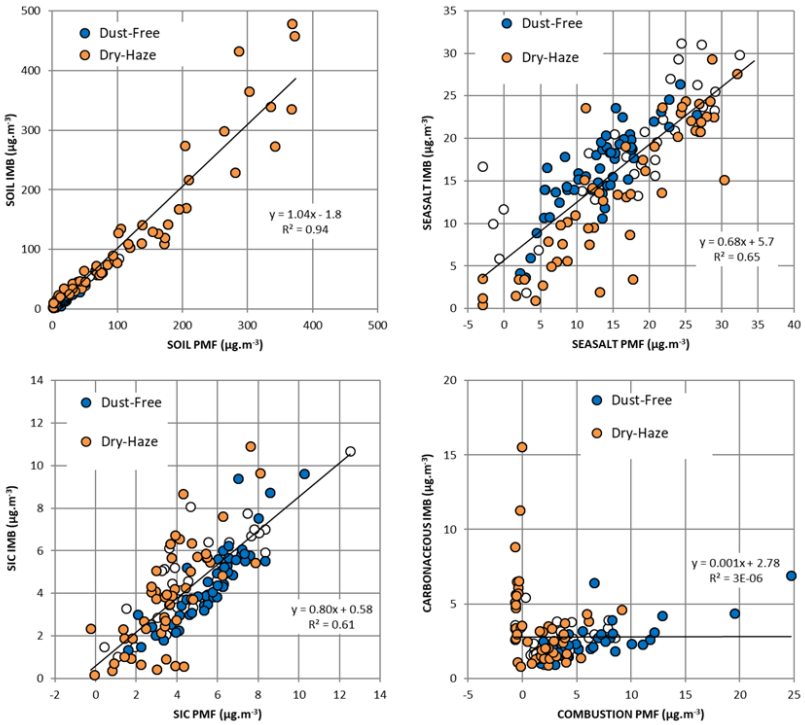

Figure 7: Comparison between the apportionment of individual samples using IMB and PMF, for four source classes. Circles filled in white represent periods with intermittent dust intrusions. Linear best fits are presented for the total sampling campaign.

Both methodologies also compare reasonably well in what concerns Secondary Inorganic Compounds (SIC) contributions to the aerosol loading, with a ratio IMB/PMF=0.80 and a correlation coefficient R=0.78. Where the comparison fails completely is in the Carbonaceous (IMB) versus Combustion (PMF) sources that present no clear relation. This results from several facts as exposed in the following text. IMB source profile represents only non-carbonate carbonaceous matter, irrespective of the source, while PMF factor intends to represent all emissions from combustion sources, besides carbonaceous matter. Therefore, from Figure 7 it is possible to observe in several samples important contributions of Carbonaceous matter estimated by IMB, while PMF gives zero to negative Combustion emission estimations. Most probably this results from soil contribution to organic matter that in PMF is attributed to dust or anthropogenic sources (Ant+Dust, see Graphs C and H in Figure A8, for clarification). Also in PMF the Combustion source has, in average, an important contribution (around 50%; see Figure A8, for

clarification) of elements, such as Si, Al, Fe, etc., from soil origin and, therefore, in our opinion, this PMF Combustion source is highly contaminated with soil, with PMF not fully capable of separating Combustion from Soil dust, due to the overwhelming presence of soil particles during dust episodes.

From Table 3 and Figure 7 we may then conclude that the IMB solution compares well with PMF for dust and SIC, but the two methods show important discrepancies for individual samples, principally in the estimation of sea salt and carbonaceous aerosol contributions.

4.6 Accuracy and Errors

IMB and PMF are subject to a number of errors that affect the precision and accuracy of the sources estimation. Fully acquainting for all errors is difficult, because some used information (bibliographic or experimental) has no available accuracy or is subject to unknown and unexpected errors. PMF applies several statistical tests to evaluate the influence of random errors and the rotational ambiguity of the obtained solution. Although these tests indicated that the PMF solution was robust they could not identify collinearity problems that resulted in the significant contamination of Combustion and Sea-salt sources with soil dust.

Both methodologies are equally affected by errors in the aerosol chemical analysis. Probably, the higher relative analytical errors are related with elements and EC evaluation, in conditions of high dust concentrations, although care was taken to sample for shorter periods during dust episodes. EC is frequently near the detection limits and it is quite difficult to fully evaluate the interference of coloured dust during the optical-thermo analytical process. This affects, in an unknown value, principally, the evaluation of the PMF Combustion source that uses EC as its principal tracer (see Figure A8 for clarification).

In IMB, there are probably four estimations where the errors influencing the source apportionment are higher: a) calculation of water sorbed in sea-salt; b) the estimation of total soil content based in factor F; c) Calculation of sea-salt Na^+; d) the estimation of organic matter from OC. It is necessary to take into account however that total errors are controlled by measured PM_{10} total mass constraint (Malm et al., (1994) use this comparison as a validation and self-consistency check for their reconstructed aerosol mass balance). Falling the sum of estimated masses within 96-98% of measured PM_{10} total mass, the individual errors are probably limited (or of opposite directions, with mutual compensation).

Estimation of water content in sea-salt depends mainly on metastable equilibrium considerations that give a water/dry sea-salt mass ratio varying from 0.4 to 1.4. An average value of 0.9 was applied in our calculations. Application of the two extreme values would vary the fractional contribution of wet sea-salt by, approximately, ±6%, ±7% or ±3%, for the total sampling campaign, the Dust-Free, or the Dry-Haze periods. It is necessary to consider, however, that by choosing the two ratio extremes the closure of the total PM mass would be affected, resulting in a maximum unaccounted mass of 16%, for the choice of a 0.4 value and a maximum over-prediction of 8%, for the choice of 1.4 ratio and therefore the correctness of these extreme values is questionable.

The calculation of the total soil dust was based in equation 3 that uses an average factor F value of 1.15. F values taken from Moreno et al. (2006) (see Table A1 in annex, for clarification) vary in the range 1.09-1.27 (standard deviation=0.21) and the

factor F for global composition is 1.05-1.06. A range of approximately 16% will result from the calculation of soil dust contribution by application of the two extreme F factors. Use of extreme F values would give a maximum unaccounted PM mass of 8% or an excess total PM mass calculation of 6%.

The Fe/Na^+ edge line methodology used to estimate Na^+ and Mg^{2+} was conservative, minimizing the subtraction from sea-salt. This was partially compensated by using minimum values and the Na^+_{ss}/Mg^{2+}_{ss} ratio in seawater. The edge line intercepts the x axe at Na^+ levels within the range of values observed for periods without significant dust intrusions, in accordance with the fact that there is always sea salt spray in this marine atmosphere (see Figure 2a, where air masses without dust intrusions are represented by a blue rectangle). The points to the right of the edge line have excess Na^+, by comparison with Fe in the edge line. This excess can have two origins: either it results from variability in the relative content of Na^+ in soil dust, or it is resultant from the variability in the contributions of sea salt. It is clear that the points at low Fe levels, within the blue rectangle, are only consequence from variability in sea salt spray loading. On the right border of the blue rectangle, a pink straight line is drawn, parallel to the Fe/Ion edge lines. As all the measured points are within both lines, this is a strong indicator that Na^+ and Mg^{2+} increase, in relation to the edge lines, result mostly from variability in sea-salt input. The real value of the errors in this methodology is difficult to establish but a change in the Fe/Na^+ edge ratio of 10% would have no visible effect in the estimation of sea-salt or soil dust, by IMB.

The estimated value for non-carbonate carbonaceous matter depends strongly from the OM/OC ratio. In literature values in the range 1.2-2.3 have been proposed. We used a ratio of 2.0 in the high end of the range because the sampling was performed at a background location, away from primary combustion sources, with plenty of time for oxidation and secondary formation. However, during dust episodes, important fractions of the organic material have a soil origin and for that less reliable information exists. As the Carbonaceous fraction in PM mass is only 2-6%, errors in OM/OC ratio have only a small effect in total mass attribution, but important errors, of the order of 40%, can result in the estimation of the Carbonaceous mass if a OM/OC ratio of 1.6 is the correct assumption, instead of 2.0.

5 Conclusions

Atmospheric aerosol was collected during one year, as PM_{10}, in air masses transported from North Africa to Cape Verde islands and submitted to total mass, elemental, ionic and carbon content analysis. Two clear different aerosol seasons were observed, one in December-February, with frequent intrusions of dust from Africa (denominated Dry-Haze), and other in May-September without direct African dust contamination (Dust-Free).

The application of IMB to the collected aerosol permitted the determination of 6 to 7 source classes: insoluble dust, soluble dust, sea-salt, secondary inorganic compounds from the reaction of atmospheric acidic precursors with sea-salt, dust and ammonia, and carbonaceous matter.

The sum of calculated components only partially closed the mass balance, being 20-30% of the measured PM_{10} total mass unaccounted. Consideration and estimation of particulate water content, based in bibliographic and thermodynamic

assumptions, permitted an almost total closure of the mass balance. This outcome is diverse from most previous mass balance studies, such those referred in the section Mass Balance Methodologies, where mass closure was only partial. Therefore the present IMB methodology permits a more well based mass account and apportionment of formation processes and sources.

During the Dry-Haze season dust contributed with around 80% to the aerosol mass loading, while in the Dust-Free period the main aerosol component was sea-salt that constituted approximately 50% of the aerosol mass.

The IMB methodology was compared with PMF results applied to the same data set. In seasonal averaged terms the outcomes of the two methodologies were comparable for the most important sources and formation processes. Comparison between individual samples showed however significant differences, principally for the sea-salt spray and the carbonaceous/combustion sources. Because of the overwhelming presence of dust in most samples, the PMF could not clearly separate dust from sea-salt sources. On the other hand, IMB could not discriminate soil organic matter from combustion emissions.

We can rely in the complementarity of both methods for the evaluation of sources contributing to atmospheric contamination, in circumstances of very high natural inputs of sea-salt and desert dust particles, subject to atmospheric transformation during long-range transport. Utilization of these two independent source apportionment methodologies adds confidence to the apportionment of an atmospheric aerosol with quite specific and uncommon characteristics.

Otherwise, source composition and contribution knowledge obtained with IMB can be used to constrain a model run with the last versions of the PMF model in order to get more refined solutions than the original ones. Constraints can be created using specific ratios between two different species or mass balance equations derived from IMB techniques such as those performed in this study.

Acknowledgements

The authors gratefully acknowledge the Portuguese Science Foundation through the project CV-DUST - Atmospheric aerosol in Cape Verde region: seasonal evaluation of composition, sources and transport (PTDD/AAC-CLI/100331/2008) and the PhD scholarship of João Cardoso. C2TN/IST/ULisboa authors gratefully acknowledge the FCT support through the UID/Multi/04349/2013 project**.**

References

Alastuey, A., Querol, X., Castillo, S., Escudero, M., Avila, A., Cuevas, E., Torres, C., Romero, P.-M., Exposito, F., García, O., Pedro Diaz, J., Dingenen, R.V. and Putaud, J.P.: Characterisation of TSP and PM 2.5 at Izaña and Sta. Cruz de Tenerife (Canary Islands, Spain) during a Saharan Dust Episode (July 2002), Atmos. Environ. 39, 4715–4728, doi: 10.1016/j.atmosenv.2005.04.018, 2005.

Almeida, S.M., Pio, C.A., Freitas, M.C,. Reis, M.A. and Trancoso, M.A.: Source apportionment of atmospheric urban aerosol based on weekdays / weekend variability: evaluation of road re-suspended dust contribution, Atmos. Environ., 40, 2058-67, doi: 10.1016/j.atmosenv.2005.11.046, 2006a.

Almeida, S.M., Pio, C.A., Freitas, M.C., Reis, M.A. and Trancoso, M.A.: Approaching $PM_{2.5}$ and $PM_{2.5-10}$ source apportionment by mass balance analysis, principal component analysis and particle size distribution, Sci. Total Environ., 368, 663-74, doi: 10.1016/j.scitotenv.2006.03.031, 2006b.

Almeida-Silva, M., Almeida, S.M., Cardoso, J., Nunes, T., Reis, M.A., Chaves, P.C. and Pio, C.A.: Characterization of the aeolian aerosol from Cape Verde by k(0)-INAA and PIXE, J. Radioanal. Nucl. Chem., 300, 2, 629-635, doi: 10.1007/s10967-014-2957-9, 2014.

Almeida-Silva, M., Almeida, S.M., Freitas, M.C., Pio, C.A., Nunes, T. and Cardoso, J.: Impact of Sahara dust transport on Cape Verde atmospheric element particles. J. Toxicol. Env. Heal. A, 76, 240-251, doi: 10.1080/15287394.2013.757200, 2013.

Almeida, S.M., Freitas, M.C., Reis, M., Pinheiro, T., Felix, P.M. and Pio, C.A.: Fifteen years of nuclear techniques application to suspended particulate matter studies, J. Radioanal. Nucl. Chem., 297, 347-356, doi: 10.1007/s10967-012-2354-1, 2013

Amato, F., Alastuey, A., Karanasiou, A., Lucarelli, F., Nava, S., Calzolai, G., Severi, M., Becagli, S., Gianelle, V.L., Colombi, C., Alves, C., Custódio, D., Nunes, T., Cerqueira, M., Pio, C., Eleftheriadis, K., Diapouli, E., Reche, C., Minguillón, M.C., Manousakas, M., Maggos, T.,Vratolis, S., Harrison, R.H. and Querol, X.: AIRUSE-LIFE+: a harmonized PM speciation and source apportionment in 5 Southern European cities, Atmos. Chem. Phys., 16, 3289-3309, doi: 10.5194/acp-16-3289-2016, 2016.

Andrews, E., Saxena, P., Musarra, S., Hildemann, L.M., Koutrakis, P., McMurry, P.H., Olmez, I. and White, W.H.: Concentration and Composition of Atmospheric Aerosols from the 1995 SEAVS Experiment and a Review of the Closure between Chemical and Gravimetric Measurements, J. Air & Waste Manage. Assoc., 50, 648-664, doi: 10.1080/10473289.2000.10464116, 2000.

Ashbaugh, L.L., Myrup, L.O. and Flocchini, R.G.: A principal component analysis of sulfur concentrations in the western United States, Atmos. Environ., 18, 783-791, doi: 10.1016/0004-6981(84)90262-2, 1984.

Blanchard, C.: Methods for attributing ambient air pollutants to emission sources, Annu. Rev. Energy Environ., 24, 329-365, doi: 10.1146/annurev.energy.24.1.329, 1999.

Belis, C.A., Karagulian, F., Larsen, B.R. and Hopke, P.K.: Critical review and meta-analysis of ambient particulate matter source apportionment using receptor models in Europe, Atmos. Environ., 69, 94-108, doi: 10.1016/j.atmosenv.2012.11.009, 2013.

Belis, C.A., Larsen, B.R., Amato, F., El Haddad, I., Favez, O., Harrison, R.M., Hopke, P.K., Nava, S., Paatero, P., Prevot, A., Quass, U., Vecchi, R. and Viana, M.: European Guide on Air Pollution Source Apportionment with Receptor Models, JRC Reference Report EUR 26080. Publication Office of the European Union, ISBN 978-92-79-32514-4, doi: 10.2788/9332, 2014.

Brunekreef, B. and Fosberg, B.: Epidemiological evidence of effects of coarse airborne particles on health, Eur. Respir. J., 26, 309-318, doi: 10.1183/09031936.05.00001805, 2005.

Buseck, P.R. and Pósfai, M.: Airborne minerals and related aerosol particles: Effects on climate and the environment, PNAS, 96, 3372-3379, doi: 10.1073/pnas.96.7.3372, 1999.

Castillo, S., Moreno, T., Querol, X., Alastuey, A., Cuevas, E., Herrmann, L., Mounkaila, M. and Gibbons, W.: Trace element variation in size-fractionated African desert dusts, J. Arid Environ., 72, 1034–1045, doi: 10.1016/j.jaridenv.2007.12.007, 2008.

Chen, X. and Yu J.Z.: Measurement of organic mass to organic carbon ratio in ambient aerosol samples using a gravimetric technique in combination with chemical analysis. Atmos. Environ., 41, 8857-8864, doi: 10.1016/j.atmosenv.2007.08.023, 2007.

Chiapello, I., Bergametti, G., Chatenet, B., Bousquet, P. and Santos Soares, E.: Origins of African dust transported over northeastern tropical Atlantic. J. Geophys. Res., 102, 13,701-13,709, doi: 10.1029/97JD00259, 1997.

Countess, R.J., Wolff, G.T. and Cadle, S.H.: The Denver Winter Aerosol: A Comprehensive Chemical Characterization, J. Air Pollut. Control Assoc., 30, 1194–1200, doi: 10.1080/00022470.1980.10465167, 1980.

Canepari, S., Farao, C., Marconi, E., Giovannelli, C. and Perrino C.: Qualitative and quantitative determination of water in airborne particulate matter, Atmos. Chem. Phys., 13, 1193-1202, doi: 10.5194/acp-13-1193-2013, 2013.

Dick,W. D., Saxena, P., and McMurry, P. H.: Estimation of water uptake by organic compounds in submicron aerosols measured during the Southeastern aerosol and visibility study. J. Geophys. Res., 105, 1471–1479, doi: 10.1029/1999JD901001, 2000.

Eldred B (2003) Internal memo to IMPROVE Staff. http://vista.cira.colostate.edu/improve/Publications/GrayLit/023_SoilEquation/Soil_Eq_Evaluation.pdf.

Eltayeb, M.A.H., Injuk, J., Maenhaut, W. and Van Grieken, R.E.: Elemental Composition of Mineral Aerosol Generated from Sudan Sahara Sand, J. Atmos. Chem., 40, 247–273, doi: 10.1023/A:1012272208129, 2001.

El-Zanan, H.S., Zielinska, B., Mazzoleni, L.R., Hansen, D.A.: Analytical determination of the aerosol organic mass-to-organic carbon ratio, J. Air Waste Manag. Assoc., 59(1), 58-69, doi: 10.3155/1047-3289.59.1.58, 2009.

Ervens, B., Turpin, B.J. and Weber, R.J.: Secondary organic aerosol formation in cloud droplets and aqueous particles (aqSOA): a review of laboratory, field and model studies, Atmos. Chem. Phys., 11, 11069–11102, doi: 10.5194/acp-11-11069-2011, 2011.

Formenti, P., Andreae, M.O., Lange, L., Roberts, G., Cafineyer, J., Rajta, I., Maenhaut, W., Holben, B.N., Artaxo, P. and Lelieveld, J.: Saharan dust in Brazil and Suriname during the Large-Scale Biosphere-Atmosphere Experiment in Amazonia (LBA) - Cooperative LBA Regional Experiment (CLAIRE) in March 1998. J. Geophys. Res., 106, 14,919-14,934, doi: 10.1029/2000JD900827, 2001.

Formenti, P., Elbert, W., Maenhaut, W., Haywood, J. and Andrea, M.O.: Chemical composition of mineral dust aerosol during Saharan Dust Experiment (SHADE) airborne campaign in the Cape Verde region, September 2000, J. Geophys Res., 108, D18, 8576, doi: 10.1029/2002JD002648, 2003.

Gama, C., Tchepel, O., Baldasano, J., Basart, S., Ferreira, J., Pio, C., Cardoso, J. and Borrego, C.: Seasonal patterns of Saharan dust over Cape Verde - a combined approach using observations and modelling, Tellus B, 67:24410, doi: 10.3402/tellusb.v67.24410, 2015.

Genga, A., Ielpo, P., Siciliano, T. and Siciliano, M.: Carbonaceous particles and aerosol mass closure in PM2.5 collected in a port city, Atmos. Res., 183,245-254, doi: 10.1016/j.atmosres.2016.08.022, 2017.

Ginoux, P., Prospero, J.M., Gill, T.E. Hsu, N.C. and Zhao, M.: Global-scale attribution of anthropogenic and natural dust sources and their emission rates based on MODIS deep blue aerosol products, Rev. Geophys., 50, RG3005, doi: 10.1029/2012RG000388, 2012.

Goodman, A.L., Underwood, G.M. and Grassian, V.H.: A laboratory study of the heterogeneous reaction of nitric acid on calcium carbonate particles, J. Geophys. Res., 105, 29,053-29,064, doi: 10.1029/2000JD900396, 2000.

Grigoratos, T., Samara, C., Voutsa, D., Manoli, E. and Kouras, A.: Chemical composition and mass closure of ambient coarse particles at traffic and urban-background sites in Thessaloniki, Greece, Environ Sci. Pollut. Res., 21, 7708-7722, doi: 10.1007/s11356-014-2732-z, 2014.

Guieu, C., Loye-Pilot, M.-D., Ridame, C. and Thomas, C.: Chemical characterization of the Saharan dust end-member: Some biogeochemical implications for the western Mediterranean Sea, J. Geophys. Res., 107, D15, doi: 10.1029/2001JD000582, 2002.

Guinot, B., Cachier, H. and Oikonomou, K.: Geochemical perspectives from a new aerosol chemical mass closure, Atmos. Chem. Phys., 7, 1657–1670, doi: 10.5194/acp-7-1657, 2007.

Harrison, R.M., Jones, A.M. and Lawrence, R.G.: A pragmatic mass closure model for airborne particulate matter at urban background and roadside sites, Atmos. Environ., 37, 4927–4933, doi: 10.1016/j.atmosenv.2003.08.025, 2003.

Henry, R.C., Lewis, C.W., Hopke, P.K. and Williamson, H.J.: Review of receptor model fundamentals, Atmos. Environ., 18, 1507-1515, doi: 10.1016/0004-6981(84)90375-5, 1984.

Hopke, P.K.: Receptor Modelling in Environmental Chemistry. Wiley & Sons, NY, 1985.

Japar, S.M., Szkarlat, A.C., Gorse, Jr. R.A., Heyerdahl, E.K., Johnson, R.L., Rau, J.A., and Huntzicker, J.J.: Comparison of Solvent Extraction and Thermal Optical Carbon Analysis Methods: Application to Diesel Vehicle Exhaust Aerosol, Environ. Sci. Technol., 18, 231–234, doi: 10.1021/es00122a004, 1984.

Journet, E., Balkanski, Y. and Harrison, S.P.: A new data set of soil mineralogy for dust-cycle modeling. Atmos. Chem. Phys., 14, 3801–3816, doi: 10.5194/acp-14-3801-2014, 2014.

Kandler, K., Schütz, L., Deutscher, C., Eber, M., Hofmann, H., Jäckel, S., Jaenicke, R., Knippertz, P., Lieke K., Massling, A., Petzold, A., Schladitz, A., Weinzierl, B., Wiedensohler, A., Zorn, S. and Weinbruch, S.: Size distribution, mass concentration, chemical and mineralogical composition and derived optical parameters of the boundary layer aerosol at Tinfou, Morocco, during SAMUM 2006, Tellus B, 61, 32–50, doi: 10.1111/j.1600-0889.2008.00385.x, 2009.

Kitamori, Y., Mochida, M., and Kawamura, K.: Assessment of the aerosol water content in urban atmospheric particles by the hygroscopic growth measurements in Sapporo, Japan, Atmos. Environ., 43, 3416–3423, doi: 10.1016/j.atmosenv.2009.03.037, 2009.

Lohmann, U. and Feichter, J.: Global indirect aerosol effects: a review, Atmos. Chem. Phys., 5, 715–737, doi: 10.5194/acp-5-715-2005, 2005.

Mirante, F., Salvador, P., Pio, C., Alves, C., Artinano, B., Caseiro, A. and Revuelta, M.A.: Size fractionated aerosol composition at roadside and background environments in the Madrid urban atmosphere. Atmos. Res., 138, 278–292. 1873-2895, doi: 10.1016/j.atmosres.2013.11.024, 2014.

Malm, W.C., Sisler, J.F., Huffman, D., Eldred, R.A. and Cahill, T.A.: Spatial and seasonal trends in particle concentration and optical extinction in the United States. J. Geophys. Res., 9, 1347-1370, doi:10.1029/93JD02916.Mason B., Moore C.B.: Principles of Geochemistry (4th ed) Wiley & Sons, 1982.

Moreno, T., Querol, X., Castillo, S., Alastuey, A. and Cuevas, E.: Geochemical variations in Aeolian mineral particles from the Sahara-Sahel dust corridor. Chemosphere, 65, 261–270, doi: 10.1016/j.chemosphere.2006.02.052, 2006.

Nenes, A., Pandis, S.N. and Pilinis, C.: ISORROPIA: A new thermodynamic equilibrium model for multiphase multicomponent inorganic aerosols, Aquat. Geoch., 4, 123–152, doi: 10.1023/A:1009604003981, 1998a.

Nenes, A., Pilinis, C. and Pandis, S.N.: Continued Development and Testing of a New Thermodynamic Aerosol Module for Urban and Regional Air Quality Models, Atmos. Env., 33, 1553–1560, doi: 10.1016/S1352-2310(98)00352-5, 1998b.

Paatero, P. and Tapper, U.: Positive matrix factorization: A non-negative factor model with optimal utilization of error estimates of data values. Environmetrics 5, 111–126, doi: 10.1002/env.3170050203, 1994.

Paatero, P.: The multilinear engine—a table-driven least squares program for solving multilinear problems, including the n-way parallel factor analysis model. J. Comput. Graph Stat., 8, 854–888, doi: 10.1080/10618600.1999.10474853, 1999.

Perrino, C., Canepari, S., Catrambone, M.: Comparing the Performance of Teflon and Quartz Membrane Filters Collecting Atmospheric PM: Influence of Atmospheric Water, Aerosol Air Qual. Res., 13, 137–147, doi: 10.4209/aaqr.2012.07.0167, 2013.

Pio, C., Cerqueira, M., Harrison, R., Nunes, T., Mirante, F., Alves, C., Oliveira, C., Sanchez de la Campa, A., Artíñano, B., and Matos, M.: OC/EC Ratio Observations In Europe: Re-Thinking The Approach For Apportionment Between Primary And Secondary Organic Carbon, Atmos. Environ., 45, 6121–6132, doi: 10.1016/j.atmosenv.2011.08.045, 2011.

Pio, C.A. and Lopes, D.: Chlorine loss from marine aerosol in a coastal atmosphere. J. Geophys. Res.,103, 25263–25269, doi: 10.1029/98JD02088, 1998.

Pio, C.A., Ramos, M.O. and Duarte, A.C.: Measurement of Carbonates in Atmospheric Aerosols by Acidification and NDIR Analysis of Evolved CO_2. In Physico-Chemical Behaviour of Atmospheric Pollutants. Edit Angeletti G. and Restelli G., Report EUR 15609/1 EN. European Commission. Brussels, Vol 1, pp 712-717, 1994.

Pope, C.A. III : Review: Epidemiological basis for particulate air pollution health standards. Aerosol Sci. Tech., 32, 4–14, doi: 10.1080/027868200303885, 2000.

Poschl, U.: Atmospheric aerosols: Composition, transformation climate and health effects, Angew Chem. Int. Ed., 44, 7520–7540, doi: 10.1002/anie.200501122, 2005.

Raes, F., Van Dingenen, R., Vignati, E., Wilson, J., Putaud, J.P., Seinfeld, J.H. and Adams, P. : Formation and cycling of aerosols in the global troposphere, Atmos. Environ., 34, 4215–4240, doi: 10.1016/S1352-2310(00)00239-9, 2000.

Ramanathan, V., Crutzen, P.J., Kiehl, J.T. and Rosenfeld, D.: Aerosols, Climate, and the Hydrological Cycle, Science, 294,2119–2124, doi: 10.1126/science.1064034, 2001.

Rees, S.L., Robinson, A.L., Khlystov, A., Stanier, C.O. and Pandis, S.N.: Mass Balance Closure and the Federal Reference Method for PM 2.5 in Pittsburgh, Pennsylvania, Atmos. Environ., 38, 3305–3318, doi : 10.1016/j.atmosenv.2004.03.016, 2004.

Reff, A., Eberly, S.I. and Bhave, P.V.: Receptor Modeling of Ambient Particulate Matter Data Using Positive Matrix Factorization: Review of Existing Methods, J. Air Waste Man. Assoc., 57, 146–154, doi: 10.1080/10473289.2007.10465319, 2007.

Remoundaki, E., Papayannis, A., Kassomenos, P., Mantas, E., Kokkalis, P. and Tsezos, M.: Influence of Saharan Dust Transport Events on PM 2.5 Concentrations and Composition over Athens, Water Air Soil Pollut. 224: 1373, doi: 10.1007/s11270-012-1373-4, 2013.

Rogge, W.F., Hildemann, L.M., Mazurek, M.A., Cass, G.R. and Simoneit B.R.T.: Sources of Fine Organic Aerosol. 4. Particulate Abrasion Products from Leaf Surfaces of Urban Plants, Environ. Sci. Technol., 27, 2700–2711, doi: 10.1021/es00049a008, 1993a.

Rogge, W.F., Mazurek, M.A., Hildemann, L.M., and Cass, G.R.: Quantifcation of Urban Organic Aerosols at a Molecular Level: Identification, Abundance and Seasonal Variation, Atmos. Environ., 27, 1309–1330, doi: 10.1016/0960-1686(93)90257-Y, 1993b.

Russel L.M.: Aerosol Organic-Mass-to-Organic-Carbon Ratio Measurements. Environ. Sci. Technol., 37 (13), 2982–2987, doi: 10.1021/es026123w, 2003.

Salvador, P., Almeida, S.M., Cardoso, J., Almeida-Silva, M., Nunes, T., Cerqueira, M., Alves, C., Reis, M.A., Chaves, P.C., Artinano, B. and Pio, C.: Composition and origin of PM10 in Cape Verde: Characterization of long-range transport episodes, Atmos. Environ., 127, 326–339, doi: 10.1016/j.atmosenv.2015.12.057, 2016.

Sciare, J., Oikonomou, K., Cachier, H., Mihalopoulos, N., Andreae, M. O., Maenhaut, W. and Sarda-Estève , R.: Aerosol mass closure and reconstruction of the light scattering coefficient over the Eastern Mediterranean Sea during the MINOS campaign, Atmos. Chem. Phys., 5, 2253–2265, doi: 10.5194/acp-5-2253-2005, 2005.

Scheuvens, D., Kandler, K., Ebert, M. and Weinbruch, S.: Bulk composition of northern African dust and its source sediments — A compilation, Earth-Sci. Rev., 116, 170–194, doi: 10.1016/j.earscirev.2012.08.005, 2013.

Seinfeld, J.H. and Pandis, S.N.: Atmospheric Chemistry and Physics: From Air Pollution to Climate Change, 2nd Edition available in Wiley, Hoboken, NJ, ISBN: 978-0471178163, 1998.

Sempere, R., and Kawamura, K.: Comparative Distributions of Dicarboxylic Acids and Related Polar Compounds in Snow, Rain and Aerosols from Urban Atmosphere, Atmos. Environ., 28:449–459, doi: 10.1016/1352-2310(94)90123-6, 1994.

Schuttlefield, J. D., Cox, D. and Grassian, V. H.: An Investigation of water uptake on Clays Minerals Using ATR-FTIR Spectroscopy Coupled with Quartz Crystal microbalance measurements, J. Geophys. Res., 112, D21303, doi: 10.1029/2007JD008973, 2007.

Speer, R. E., Barnes, H. M., and Brown, R.: An instrument for measuring the liquid content of aerosols, Aerosol Sci. Technol., 27, 50–61, doi: 10.1080/02786829708965457, 1997.

Speer R.E., Edney E.O. and Kleindienst T.E.: Impact of organic compounds on the concentrations of liquid water in ambient $PM_{2.5}$, Aerosol Science, 34, 63–77, doi: 10.1016/S0021-8502(02)00152-0, 2003.

Stanier, C., Khlystov, A., Chan, W. R., Mandiro, M., and Pandis, S. N.: A method for the in-situ measurement of aerosol water content of ambient aerosols: The Dry-Ambient Aerosol Size Spectrometer (DAASS), Aerosol Sci. Technol., 38, 215-228, doi: 10.1080/02786820390229525, 2004.

Tanaka, T.Y. and Chiba, M.: A numerical study of the contributions of dust source regions to the global dust budget. Global Planet Change, 52, 88-104, doi: 10.1016/j.gloplacha.2006.02.002, 2006.

Tang, I.N., Munkelwitz, H.R.: Water activities, densities, and refractive indices of aqueous sulfates and sodium nitrate droplets of atmospheric importance. J. Geophys. Res., 99, 18801–18808, doi: 10.1029/94JD01345, 1994.

Tang, I.N., Tridico, A.C. and Fung, K.H.: Thermodynamic and optical properties of sea salt aerosols. J. Geophysical Res., 102, 23,269-23,275, doi: 10.1029/97JD01806, 1997.

Tobias, A., Perez, L., Diaz J., Linares, C., Pey, J., Alastuey, A., Querol, X.: Short term effects of particulate matter on total mortality during Saharan dust outbreaks: a case-crossover analysis in Madrid (Spain), Sci. Total Environ. 412–413, 386-389, doi: 10.1016/j.scitotenv.2011.10.027, 2011.

Turekian, K.K.: Oceans. Prentice-Hall, 1968.

Turpin, B.J. and Lim, H.J.: Species Contributions to PM 2.5 Mass Concentrations: Revisiting Common Assumptions for Estimating Organic Mass, Aerosol Sci. Technol., 35, 602–610, doi: 10.1029/97JD01806, 2001.

Tsyro, S.G.: To what extent can aerosol water explain the discrepancy between model calculated and gravimetric PM 10 and PM 2.5, Atmos. Chem. Phys. 5, 515–532, doi: 10.5194/acp-5-515-2005, 2005.

Watson, J.G., Zhu, T., Chow, J.C., Engelbrecht, J., Fujita, E.M. and Wilson, W.E.,: Receptor modeling application framework for particle source apportionment. Chemosphere, 49, 1093-1136, doi:10.1016/S0045-6535(02)00243-6, 2002.

Wedepohl, K.H.: The composition of the continental crust. Geochim. Cosmochim. Ac., 59, 1217-1232, doi: 10.1016/0016-7037(95)00038-2, 1995.

Xu, J., Imre, D., McGraw, R. and Tang, I.: Ammonium sulphate: Equilibrium and metastability phase diagrams from 40 to -50 ºC. J. Phys. Res. B, 102, 7462–7469, doi: 10.1021/jp981929x, 1998.

ANNEX

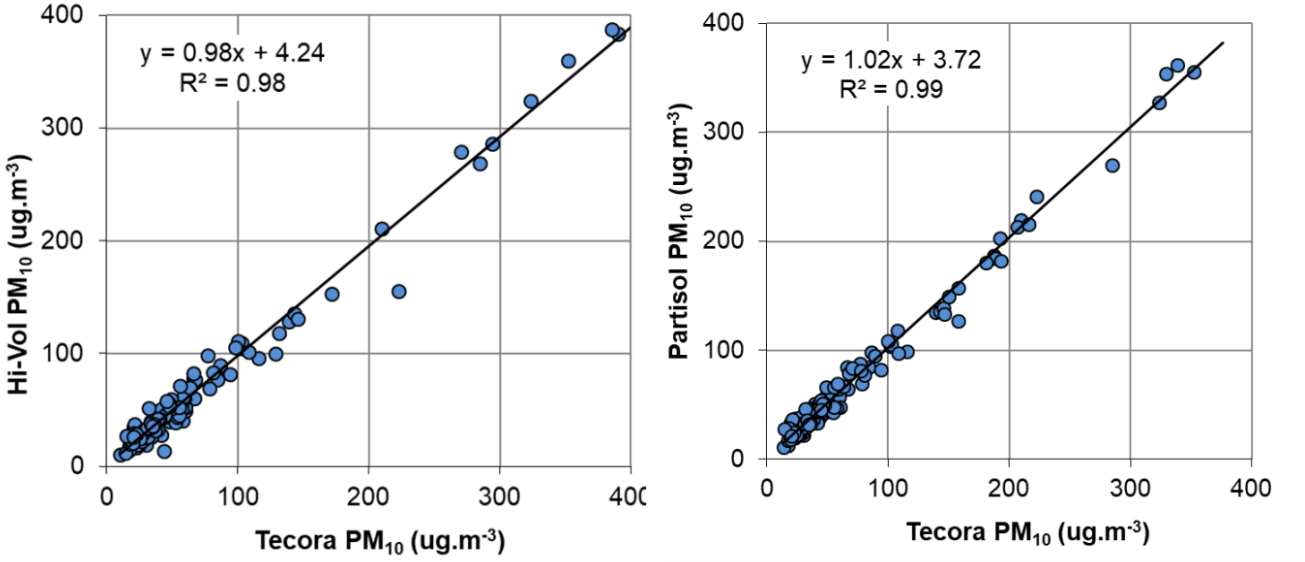

Figure A1: Comparison between PM_{10} concentration values, in atmospheric aerosol parallel sampling with Nuclepore (Tecora), Teflon (Partisol) and Quartz (Hi-Vol) filters.

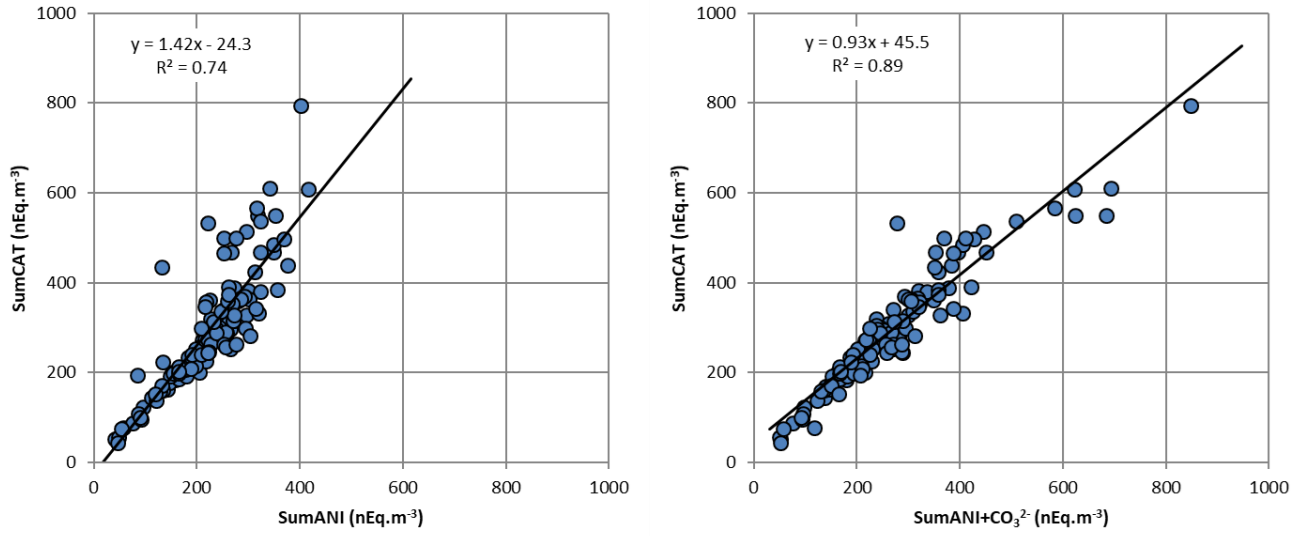

Figure A2: Ion balance between total analysed cations and anions, without and with the inclusion of measured carbonates (ANI- anions; CAT- cations).

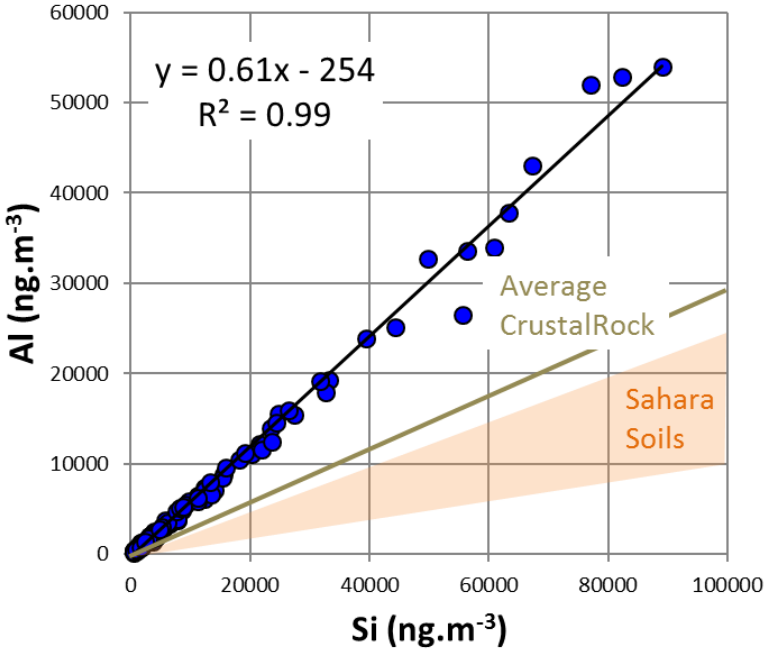

Figure A3: Relation between Si and Al concentrations in atmospheric aerosols. Also shown Al/Si ratio ranges, in Sahara, and average value for global soils, taken from Moreno et al., (2006), and Manson and Moore, (1982), respectively.

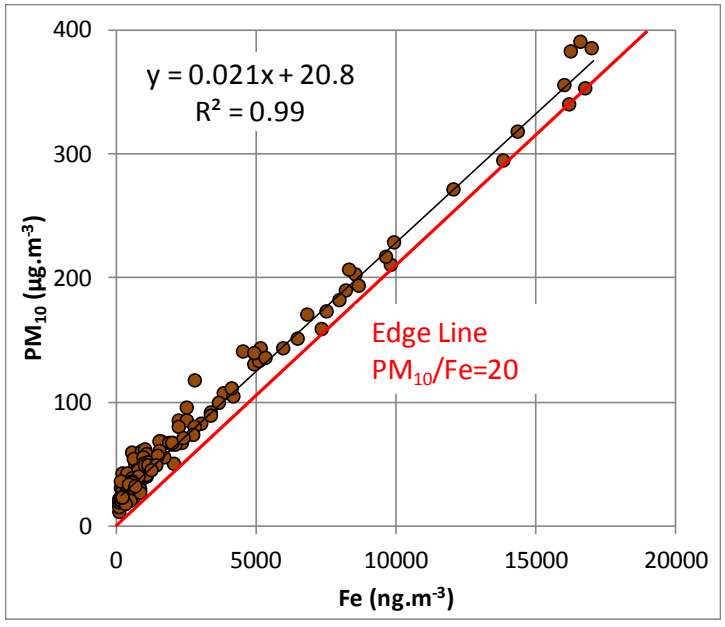

Figure A4: Relation between Fe and PM_{10} concentrations. The red line is the low edge representing, approximately, the amount of dust in PM_{10}

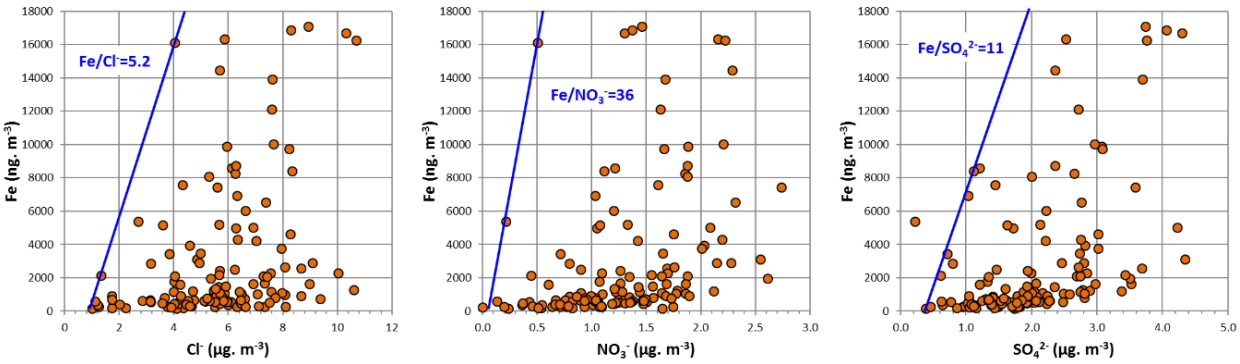

Figure A5: Edge lines for chloride, nitrate and sulphate, representing, coarsely, the amount of these anions in soil dust.

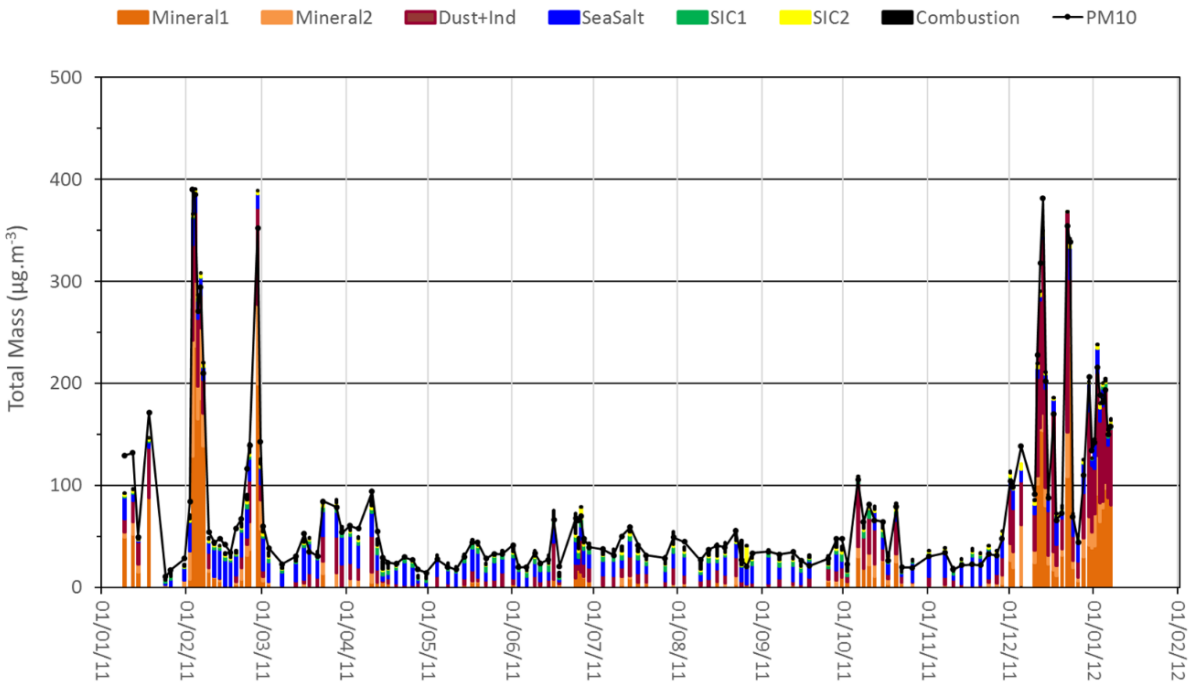

Figure A6: Source contributions for individual sampling events, calculated with PMF

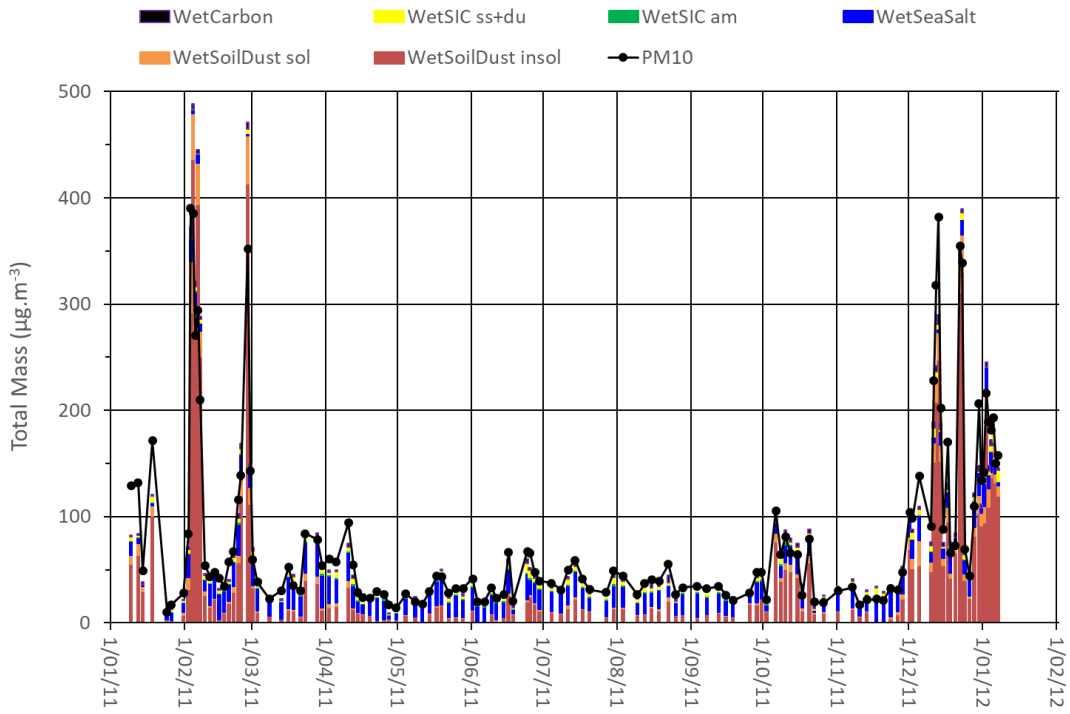

5 Figure A7: Source contributions for individual sampling events, calculated with the IMB methodology.

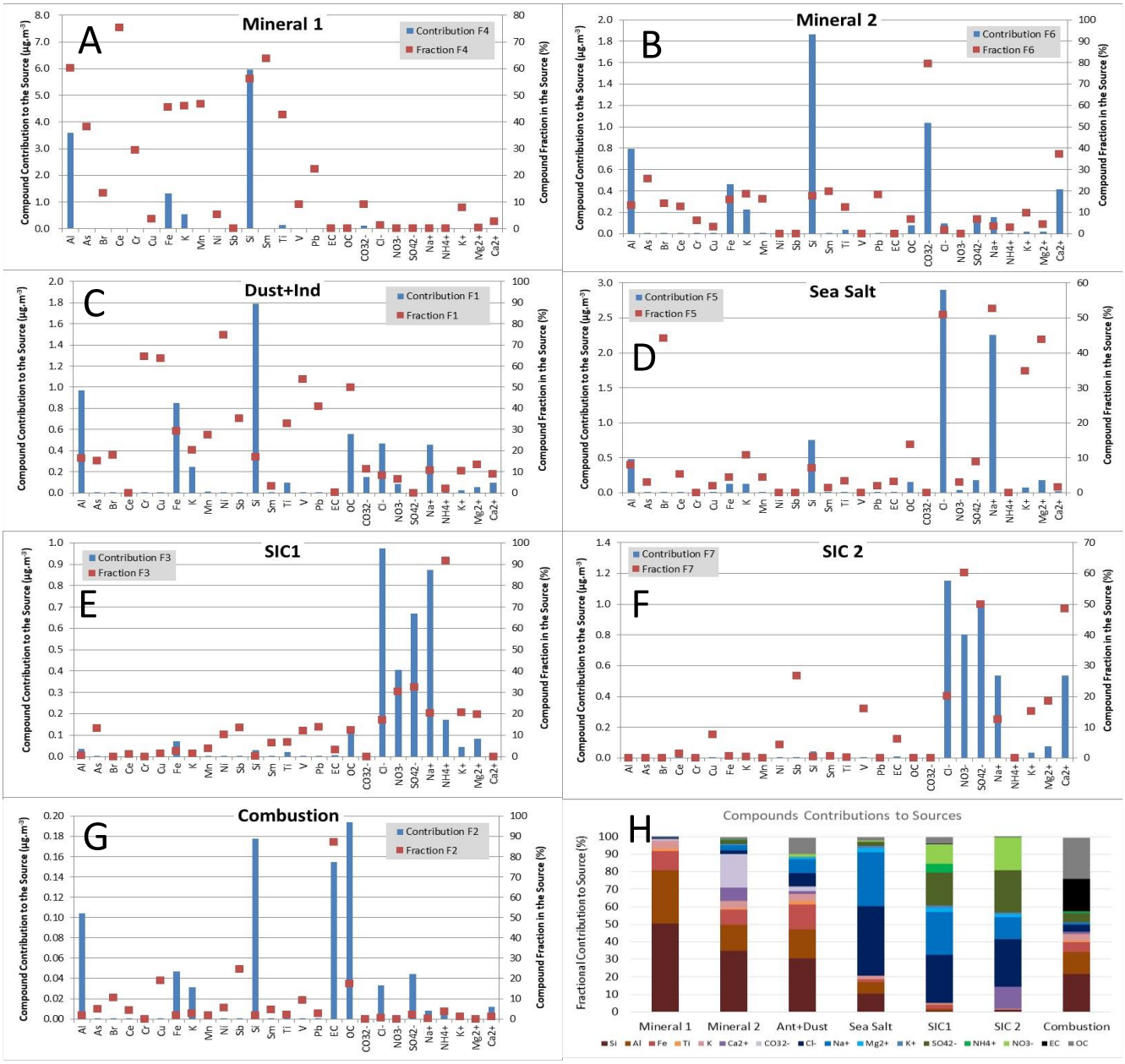

Figure A8: PMF Source Contributions and Profiles for the seven identified factors (Graphs A-G). Graph H presents the fraction contribution of each main compound to each source.

Table A1: Concentrations of major elemental species (as oxides) at nine sites in Sahara region, according to Moreno et al., (2006), and average crustal levels taken from Manson and Moore, (1982). The table presents also the estimation of factor F used in Equation 3.

	CrustalAver	Hoggar Massif		Chad Basin		Niger		Western Sahara			Sahara
		HM1	HM2	CB1	CB2	MON	HAR	WS1	WS2	WS3	Average
	(%)	(%)	(%)	(%)	(%)	(%)	(%)	(%)	(%)	(%)	(%)
SiO_2	59.3	62.1	62.5	63.2	70.2	69.5	66.7	49.4	46.2	56.8	60.7
TiO_2	0.7	1.4	1.2	1.0	1.2	1.4	1.2	0.6	0.4	0.9	1.0
Al_2O_3	15.4	14.7	13.6	14.0	11.7	11.6	12.2	8.8	7.0	5.1	11.0
Fe_2O_3	7.2	6.1	5.2	6.7	4.7	4.4	5.7	4.4	2.8	4.2	4.9
MnO	0.1	0.1	0.1	0.0	0.1	0.0	0.1	0.1	0.1	0.1	0.1
MgO	3.5	1.8	1.6	1.2	0.8	0.5	0.9	2.9	2.6	1.9	1.6
CaO	5.1	2.4	2.0	1.4	1.4	0.4	1.6	12.9	17.7	12.2	5.8
K_2O	3.1	2.5	2.5	1.5	1.5	1.2	1.8	1.9	1.7	1.4	1.8
SUM	**94.4**	**91.0**	**88.6**	**89.0**	**91.5**	**88.9**	**90.1**	**80.9**	**78.5**	**82.6**	**86.8**
Na_2O	3.8	1.6	1.9	1.1	0.5	0.4	0.6	0.9	0.7	0.8	0.9
P_2O_5	3.1	2.5	2.5	1.5	1.5	1.2	1.8	1.9	1.7	1.4	1.8
SO_3	0.1	0.2	0.2	0.3	0.2	0.0	0.1	0.1	0.1	0.1	0.1
TOTAL	**98.5**	**93.1**	**91.0**	**90.6**	**92.3**	**89.4**	**91.0**	**82.2**	**79.7**	**83.9**	**88.1**

F=100/86.8= 1.15